AD-A179 217   THE PERCEPTION OF BRIGHTNESS AND COLOUR;   1/1
              NEUROPHYSIOLOGY PSYCHOPHYSICS AND COMPUTATION(U) OXFORD
              UNIV (ENGLAND) DEPT OF PHYSIOLOGY A J PARKER ET AL.
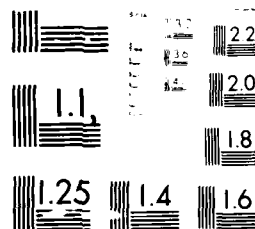UNCLASSIFIED 27 FEB 87 KK-8F-161 AFOSR-85-0296   F/G 6/16   NL

END
DATE
FILMED
5-87

AD-A179 217

FINAL SCIENTIFIC REPORT: AFOSR-85-0296
27th February 1987

The Perception of Brightness and Colour:
Neurophysiology, Psychophysics and Computation.

A.J. Parker, M.J. Hawken, C.B. Blakemore
University Laboratory of Physiology,
Parks Road, Oxford, OX1 3PT, England, UK

Final Scientific Report, 1 Oct 1986 to 30 Sep 1987

Approved for public release; distribution unlimited.

Prepared for

US Air Force, Det 1, 76 ALD/ACFMCC,
Bolling AFB DC 20332-5260

and

European Office of Aerospace Research and Development,
London, UK.

AFR 1 7 1987

A

87

REPORT DOCUMENTATION PAGE

1a. REPORT SECURITY CLASSIFICATION		1b. RESTRICTIVE MARKINGS		
UNCLASSIFIED				
2a. SECURITY CLASSIFICATION AUTHORITY		3. DISTRIBUTION/AVAILABILITY OF REPORT		
2b. DECLASSIFICATION/DOWNGRADING SCHEDULE		Approved for public release; distribution unlimited		
4. PERFORMING ORGANIZATION REPORT NUMBER(S)		5. MONITORING ORGANIZATION REPORT NUMBER(S)		
KK 8F 161		EOARD-85-0056 AND AFOSR085-0296		
6a. NAME OF PERFORMING ORGANIZATION	6b. OFFICE SYMBOL (If applicable)	7a. NAME OF MONITORING ORGANIZATION		
University of Oxford		Air Force Office of Aerospace Research and Development (EOARD)		
6c. ADDRESS (City, State, and ZIP Code)		7b. ADDRESS (City, State, and ZIP Code)		
Department of Physiology Parks Road Oxford OX1 3PT		Box 14 FPO New York 09510		
8a. NAME OF FUNDING/SPONSORING ORGANIZATION	8b. OFFICE SYMBOL (If applicable)	9. PROCUREMENT INSTRUMENT IDENTIFICATION NUMBER		
EOARD	LRB	FL2878-85-00014		

8c. ADDRESS (City, State, and ZIP Code)	10. SOURCE OF FUNDING NUMBERS			
	PROGRAM ELEMENT NO.	PROJECT NO.	TASK NO.	WORK UNIT ACCESSION NO.
Box 14 FPO New York 09510	61102F	2301	D1	199

11. TITLE (Include Security Classification)
The Perception of Brightness and Colour: Neurophysiology, Psychophysics and Computation.

12. PERSONAL AUTHOR(S)
A.J. Parker, M.J. Hawken, C.B. Blakemore

13a. TYPE OF REPORT	13b. TIME COVERED	14. DATE OF REPORT (Year, Month, Day)	15. PAGE COUNT
Final Scientific Rpt.	FROM 1Sep85 TO 31Aug86	87/02/27	68

16. SUPPLEMENTARY NOTATION

17.	COSATI CODES		18. SUBJECT TERMS (Continue on reverse if necessary and identify by block number)
FIELD	GROUP	SUB-GROUP	Visual cortex; receptive field; computational neuroscience

19. ABSTRACT (Continue on reverse if necessary and identify by block number)

Progress in research in 3 areas of computational visual neuroscience is summarized. The first project has assessed the receptive field organization of neurons in the primate striate cortex. A new model is proposed for cortical receptive fields based on linear combinations of difference-of-Gaussian functions. A detailed study of the evidence leading to this conclusion is provided in the attached pre-print of a paper which will appear in Proc. R. Soc. Lond. B, 231 (July 1987). The second project is directed towards measuring the chromatic properties of cortical cell receptive fields. The third project is assessing current computational models of the perception of 3-dimensional surfaces using psychophysical techniques with human observers.

20. DISTRIBUTION/AVAILABILITY OF ABSTRACT	21. ABSTRACT SECURITY CLASSIFICATION	
☐ UNCLASSIFIED/UNLIMITED ☐ SAME AS RPT ☐ DTIC USERS	UNCLASSIFIED	
22a. NAME OF RESPONSIBLE INDIVIDUAL	22b. TELEPHONE (Include Area Code)	22c. OFFICE SYMBOL
Maj James N. McDougal	01-4090-4285	EOARD/LRB

DD FORM 1473, 84 MAR

83 APR edition may be used until exhausted
All other editions are obsolete

SECURITY CLASSIFICATION OF THIS PAGE

INTRODUCTION

In order to illustrate the operation of neural structures in early visual processing, Robson (1980) proposed the concept of a 'neural image': this is a spatial map of the nervous activity resulting from the response of the visual system to a specific image. A very similar construct, termed a representation, was developed by proponents of the computational approach to vision (Marr, 1982; Horn, 1986). Marr (1982) argued that the function of a particular representation is to make specific kinds of information explicit. From the computational point of view, the role of early vision is to create representations that are useful for later stages of processing such as stereo or motion analysis (Mayhew and Frisby, 1981; Marr and Poggio, 1979; Hildreth, 1984).

Our programme of research is a study of how the nervous system of primates creates and uses representations of visual information. Three components are necessary in such a study. First, the behavioural performance that reflects visual information processing should be measured. This involves the construction of psychophysical experiments designed to find the limits of visual performance and to see whether distinct analysing mechanisms can be identified. Second, neurophysiological experiments should be carried out to examine how behavioural performance is supported by particular neural mechanisms. After the identification of such mechanisms, they should be characterised in greater detail and a formal description of their properties should be made. This description can be related back to the nature of the analyzing mechanisms obtained from psychophysical experiments and forward to the final goal of the research, which is the creation of a formal model in the computational sense. Thus, the third stage is for the results obtained from biological visual systems to be embodied in a computer model and the performance of the biologically-derived model to be analysed and compared with models derived from other sources, such as artificial intelligence and computer vision.

Our current work consists of three specific projects that have been designed within the framework of this general programme. The first project is investigating computable models of striate cortical receptive fields, which are the neural mechanisms responsible for the earliest transformation of the visual image at a cortical level. The second project is extending the measurements of cortical cells from the luminance contrast domain to include chromatic sensitivity. The new experiments are designed to validate the model generated in the first project and point the way to creating a computational model of chromatic processing based on primate vision. The third project is applying the general program outlined above to the study of a higher order perceptual process, namely the perception of visual surfaces by human observers. In this field, there are a number of interesting computational models derived from artificial intelligence, but there is very little information on human perception against which to evaluate these models.

The present state of progress on each of these projects is outlined in the sections that follow. More detailed accounts of the work will be submitted to AFOSR in the form of scientific papers as the work approaches completion. An appendix is attached giving details of work in preparation, as well as an account of the scientific activities of the principal investigators during the tenure of the grant. These three scientific projects are underpinned by a fourth project,

which is intended to provide a complete revision of the software used for the real-time acquisition of data during experiments.

1. COMPUTABLE MODELS OF STRIATE CORTICAL RECEPTIVE FIELDS

In this project, we are studying the initial transformations of the grey-level image that occur in primate visual systems. This involves the creation of a computable model of early visual processing, based on our quantitative measurements of the properties of single neurons in the monkey visual cortex. Our work involves comparing the performance of this model against those of others, some of which derive from experimental investigations similar to our own (Wilson and Bergen, 1979; Marcelja, 1980; Daugman, 1985; Watt and Morgan, 1984), others of which have been proposed as methods in computer vision systems (Witkin, 1983; Yuille and Poggio 1985; Shanmugam, Dickey and Green, 1979; Canny, 1983; Marr and Hildreth, 1980; Mayhew and Frisby, 1981).

Background

There is extensive evidence favouring a multiple-channel model of the detection of luminance contrast by human observers. The need for a multiple-channel model (Graham and Nachmias, 1971; Graham, Robson and Nachmias, 1978), the nature of the detection process (Robson and Graham, 1981) and the parameters of individual channels (Blakemore and Campbell, 1969) have all been analyzed quantitatively by psychophysical experiments. Further support for a multiple-channel organization has come from neurophysiological investigations in the striate cortex of cats and monkeys, where it has been shown that cells are tuned to distinctly different spatial frequencies (Cooper and Robson, 1968), even when care is taken to analyze the neurons serving a unique location in the visual field (DeValois, Albrecht and Thorell, 1982).

However, there are no detailed studies comparing the performance of biologically-derived models of detection, with different spatial weighting functions, on these fundamental tasks. In fact, many important parameters of the historical models remain unspecified. Even simple parameters like bandwidth are very difficult to estimate from psychophysical experiments (Graham, 1977; Henning, Hertz and Hinton, 1981), whilst specifying the shapes of channels or their spatial distribution is even more problematic. As a consequence, many models of human vision make assumptions about these variables, which, although they are chosen shrewdly, are nonetheless unsupported by experimental evidence (Watson, 1983; Wilson and Bergen, 1979; Sakitt and Barlow, 1982). Even though the results of neuro- physiological experiments can be difficult to interpret, they offer one possible route away from this impasse, because they provide more direct measurements of the internal working of the visual system.

Current Programme of Investigation

There is considerable evidence to suggest that the neural locus of the channels identified in psychophysical experiments is the striate cortex. For the past 3 years, we have been investigating the relationship between the performance of single neurons in the striate cortex of Old World monkeys and human observers in a number of psychophysical tasks (Parker and Hawken, 1985; Hawken and Parker,

1984; Parker and Hawken, 1983, Hawken and Parker, 1987abc, Parker and Hawken, 1987). One of the requirements of these investigations was the development of an adequate model of the receptive field of a cortical cell and the estimation of the parameter values of the model for each cell that was recorded. In order to make comparison with psychophysics more exact, the threshold contrast sensitivity of cells was measured by determining the stimulus contrast required to cause a statistically significant change in the output of the nerve cell (Parker and Hawken, 1985; Derrington and Lennie, 1982; Derrington and Lennie, 1984), over the range of spatial frequencies to which the neuron responded. These results provide a spatial contrast sensitivity function against which we can test various functions proposed for describing the spatial bandpass filters in early visual processing. In particular, we have tested the Gabor function (Marcelja, 1980; Daugman, 1985), the first differential of a Gaussian, which is a close approximation of Canny's optimal filter (Canny, 1983), and the second differential of a Gaussian (Marr and Hildreth, 1980; Watt and Morgan, 1984; Mayhew and Frisby, 1981). All these functions give rather poor descriptions of most monkey cortical cells, as illustrated by the examples in the attached manuscript. Certainly, none of these functions would allow the adoption of a single model describing all simple cells.

An alternative approach is to ask how well are the cortical cells described by combinations of functions that are known to describe the properties of receptive fields at earlier stages in the visual system (Enroth-Cugell and Robson, 1966; Rodieck, 1965). Therefore, we have studied models based on difference of Gaussians functions (DOG) and linear combinations of DOG functions. The most general case that we considered consists of 3 DOG functions, whose peaks are spatially separated from one another. In most cases, the description of the data obtained by linear combinations of single DOG functions (with a small spatial separation of their centres) is significantly better than either of the computational models that were tested (Hawken and Parker, 1987).

One of the main aims of this project is to characterise further the merits of the DOG-based functions as the basis of models in spatial vision. To accomplish this we are constructing a program to analyse natural images. Using this algorithm will enable us to compare the performance of the DOG-based spatial filters against other filters proposed in the literature (V²G, Gabor), on tasks such as the detection and localisation of edges, measurement of the local orientation and curvature of edges and the extraction of other spatial primitives.

2. CHROMATIC PROPERTIES OF SINGLE CORTICAL NEURONS

Background

Our interest in the chromatic properties of cortical cells has arisen from investigations of the functional microstructure of the monkey striate cortex. In particular we have shown that within lamina IV there is a physiological correlate of the differential anatomical distribution of afferents from magno- and parvocellular of the lateral geniculate nucleus (Hawken and Parker, 1984). We also have unpublished quantitative data on the spatial and other properties of neurons encountered within those patches of layers II and III that stain densely for cytochrome oxidase (Hendrickson, Hunt and Wu, 1981; Horton and Hubel, 1981). So

far, the published physiological investigations of cytochrome oxidase spots suggest that these spots consist of groups of cells with chromatic organization of their receptive fields, including so-called "double-opponent" cells, and weak or non-existent orientation tuning (Livingstone and Hubel, 1984).

Proposed Research

For quantitative measurements, we intend to adopt an approach derived from the psychophysical studies of Krauskopf, Williams and Heeley (1982), which indicates the existence of so-called cardinal directions in colour space. This method provides an analysis of neural responses similar to that of Rushton's method of silent substitution and has been used to considerable effect by Derrington, Krauskopf and Lennie (1984) to study the chromatic properties of neurons in macaque LGN. The stimuli consist of spatial sinusoidal waveforms whose modulations can be represented in a three colour dimensional space, two dimensions of which correspond to a plane representing the CIE chromaticity diagram and the third representing the familiar dimension of luminance contrast.

Initial experiments will include an investigation of the chromatic properties of neurons in layer IV. A detailed investigation will be made of the cells in IVc in an attempt to verify our previous conclusions (Hawken and Parker, 1984) based on the study of properties with luminance contrast alone. We will also record from cells in other layers in the striate cortex and eventually extra-striate cortex, especially those regions of layers II and III in areas V1 and V2 rich in cytochrome oxidase enzyme activity, in order to compare the chromatic and spatial organization of the receptive fields from these anatomically differentiated zones. It is possible that independent processing of chromatic and non-chromatic information seen at the level of the LGN is preserved through several higher levels of visual processing, even though both types of cells, chromatic and luminance-sensitive, may acquire new properties at the cortical level, such as orientation selectivity and binocularity. However, Zeki's work in V4 (Zeki, 1980) suggests that some transformation of the chromatic components of LGN signals eventually takes place.

Hawken and Parker (1987) describe a new computational model of the spatial organization of the receptive fields of cortical cells. One means of extending the testing of this model is to note the strong interrelationships that exist between luminance contrast sensitivity and chromatic contrast sensitivity in the LGN (Wiesel and Hubel, 1965; Derrington et. al., 1984). These interrelationships must leave their mark on cortical processing and imply that models, such as ours, which are based on discrete inputs from LGN receptive fields to the receptive subunits of cortical cells, will exhibit a degree of spatial organization of chromatic sensitivity that is different from that in the LGN. However, the DOG-based models do imply that the chromatic sensitivity of cortical cells and their luminance contrast sensitivity should be related in a unified manner.

Work in Progress

A computer-driven pattern generator has been constructed to provide independent signals to each of the three channels of a colour CRT monitor. The principle of the design is close to that used on many computer graphics systems currently available and consists of some RAM and colour look-up tables that can

be loaded from the computer, as well as the synchronization signals and output stages necessary to drive the colour monitor. The main difference from commercially available systems is that output from the device can be specified with 12-bit accuracy (1 part in 4096) on all three colour channels. This is necessary in order to achieve a wide dynamic range of contrast, as well as using the look-up tables to correct for any nonlinearity in the performance of the colour monitor. This generator can be programmed to store bars, step-edges, sinusoidal gratings or other 1-dimensional spatial profiles as a list of numbers, whose values can be interpreted as locations on an effectively continuous contour in tridimensional colour space. The software to control this device will be integrated into the general-purpose real-time control software that is being written for our research group by the Department's Computer Officer (Mr K. Stratford), who has been partially supported by AFOSR during the course of this grant.

3. COMPUTATIONAL STUDIES OF THE PERCEPTION OF VISUAL SURFACES

There is a relative scarcity of experimental investigations of how human observers abstract information about the geometric properties of visual surfaces. In order to elucidate the important geometrical factors in surface perception we are currently performing a series of psychophysical experiments. This knowledge is a prerequisite to evaluation of computational models of surface perception and to the design of neurophysiological experiments to investigate the neural populations responsible for this aspect of human perception.

A. Sensitivity for the Fundamental Geometric Properties of Surfaces

Several computational schemes assume it is relatively easy for the system to compute some simple intrinsic properties of the depth map. For example, in order to find discontinuities, Ponce and Brady's (1985) procedure first smooths the surface with Gaussian filters of various space constants and computes the principal directions and curvatures over the surface and then marks zero-crossings and extrema of the dominant curvatures. Our discrimination experiments have been carried out using surfaces embedded in random-element stereo pairs to measure the sensitivity of observers to (a) Gaussian curvature, (b) principal values of normal curvature, (c) orientation at the axes of the principal curvatures. Initial results indicate that human observers are sensitive to differences of the curvature of surfaces, independent of other possible confounding cues such as surface extent and gradient (Johnston and Parker, 1987).

B. Detection and Identification of Discontinuities in Visual Surfaces

Background

In psychophysical studies of human vision, procedures such as adaptation, masking and sub-threshold summation are used to reveal mechanisms tuned to specific regions of the stimulus domain (Braddick et al., 1978). Adaptation (Tyler, 1975; Schumer and Ganz, 1979a), masking (Tyler and Julesz, 1978) and sub-threshold summation (Schumer and Ganz, 1979a) have already been used to study stereoscopically generated surfaces that were modulated sinusoidally in depth. However, an important point made by Ponce and Brady (1985) is that knowledge of the qualitative type of a surface discontinuity is highly significant in later processing. This suggests that it may be more revealing to study a task where the

observer is required to identify a stimulus as well as detect it. Such a task was used by Krauskopf and Srebro (1965) to study colour mechanisms, by Watson and Robson (1981) to study spatial and temporal channels and by Watson et al. (1980) to study motion sensitivity. The basic presumption of this approach is that if two stimuli are each at their own detection threshold and if they can be reliably identified or discriminated, then they are being detected by separate and independent mechanisms. By studying a range of stimuli exhaustively, one can obtain a parsimonious estimate of the number and type of analysing mechanisms possessed by human observers.

Work in Progress

Random-element stereo-pairs containing these patterns defined as changes in disparity are generated (Julesz, 1971). A two-alternative forced-choice (2AFC) procedure is used to measure the detectability of these stimuli: (i) as a function of the size of the discontinuity (i.e the change in surface height in the case of a step), (ii) as a function of the contrast required to detect a given fluctuation in the surface and (iii) as a function of the degradation of stereo information when random non-corresponding elements are added to the stereo pair. During the detection task, stimuli belonging to two or more classes of discontinuity can be randomly interleaved from trial to trial and observers will classify the stimulus after each detection decision. By way of example, if the detectability of, say, step stimuli of fixed height were measured as a function of contrast, observers would be asked to discriminate between just detectable stimuli of different height but the same disparity sign; if they can do so, this would imply separate analysing mechanisms for different sizes of discontinuity, as suggested by the adaptation experiments of Blakemore and Julesz (1971). On the other hand, an ability to discriminate only crossed vs. uncrossed disparities regardless of size would support the contention of Richards (1971) that there is a limited number and distribution of disparity detectors. Using these techniques, preliminary results suggest that surfaces of positive and negative Gaussian curvature are analysed independently by human psychophysical observers.

C. Disparity Averaging and Surface Interpolation

There are several studies indicating that, in human stereo vision, low spatial frequency sinusoidal variations in depth are handled separately from high frequency ones; the filter shape for each "depth channel" would correspond roughly to a difference-of-Gaussians (DOG) function (Tyler, 1975; Tyler and Julesz, 1978; Schumer and Ganz, 1979a). This may be an analog of the multi-resolution methods for surface interpolation proposed by Terzopoulos (1984), who, however, pointed out that smoothing of surfaces with DOG filters must be carefully controlled in the vicinity of discontinuities, otherwise crucial information will be smoothed away altogether. This suggests that the space constant for smoothing may depend on the characteristics of the surface.

One phenomenon that we are exploiting to estimate the space constant of a smoothing process is disparity averaging (Kaufman et al., 1973; Foley, 1976; Julesz and Schumer, 1981). A random-dot stereo-pair is created in which alternate rows or columns of dots are used to define different visual surfaces. Schumer and Ganz (1979b) report that a composite figure consisting of a planar surface at zero disparity plus a sinusoidal modulation of depth is indistinguishable at

threshold from a single surface sinusoidally modulated at half the amplitude of depth variation. Our data extend these results to suprathreshold stimuli such as pairs of simple planar surfaces, both frontoparallel and tilted, at a variety of disparities relative to the background (Yang and Parker, 1987). In future experiments, the surfaces will be a plane and a step-edge; by making the plane terminate at various distances from the discontinuity at the step-edge, the spatial edge-weighting function for disparity averaging can be measured. Similar measures will be carried out for other types of discontinuity. An alternative way of measuring the space constant of the pooling process is to substitute for the plane a stimulus consisting of the first differential of a Gaussian with its zero-crossing located at the step-edge. Discrimination can be measured as a function of the space-constant of this Gaussian.

D. Current Organization of the Project

This work is partially supported by a grant from the UK Science and Engineering Research Council to AJP. This grant has provided a SUN-3 computer workstation to carry out this research. Considerably more extensive computing facilities have been provided by a grant from the Wellcome Trust. Since Brady is now basing his work in Oxford around SUN computer systems, the computational modelling part of the project will be carried out using this system. Experiments can be carried out either with the SUN system or with the display system provided by this grant. More recently, a grant has been awarded from funds supplied by central government to the University of Oxford for apparatus to monitor human eye movements during the inspection of visual surfaces. Experiments on detection and identification of surface properties will be carried out by Ms E. Johnston as part of her project work for her D.Phil degree. Experiments on disparity averaging are being carried out by AJP and Ms Yang Yuede (supported by a Fellowship from the Wellcome Trust).

The direction of this work changed during the course of the previous USAF grant. In that proposal, it was suggested that an initial study should focus on depth cues from luminance and texture gradients. These questions have been set aside temporarily in order to concentrate on subjects within the perception of surfaces in the domain of stereo depth. Random dot stereograms (Julesz, 1971) give relatively pure cues to surface orientation and allow convenient manipulation of these cues. Also, the phenomenon of disparity averaging observed in stereo vision can be used as an experimental probe to find out how local depth measurements are be combined to yield an integrated percept of a surface in depth. Finally, computational models for recovering surface properties from luminance gradients (e.g. Pentland, 1982) require the measurement of the second directional derivative of a Gaussian filtered version of the grey-level image. It would be natural to suppose that orientation-specific neurons in the striate cortex would fulfil this role in the primate visual system. However, a quantitative analysis of our recordings from foveal striate cortex in monkeys shows that hardly any cells are accurately described as spatial filters with a derivative of a Gaussian characteristic (Hawken and Parker, 1987).

4. REAL-TIME EXPERIMENTAL CONTROL SOFTWARE.

A computer-based system for the control and monitoring of neurophysiological and psychophysical experiments in real-time has been specified. The following

description of the current state of this project has been prepared by Mr. K. Stratford, who has been employed part-time on this grant. The significant feature is that differences amongst computer systems by using a system configuration file to define the hardware interfaces, as well as a system shell to define the user interface. Both WIMP and menu-driven shells have been implemented on an IBM PC AT under MS-DOS, while preliminary code has been written for a PDP 11/34 under RT11.

In order that the system be useful to users of various levels of expertise, various levels of access are available into the system. The expert user specifies an experiment using a combination of native C routines and a state-control language (SCL) which facilitates the definition of the particular protocol to be adopted. A formal grammar for the SCL has been defined, and the recursive-descent compiler for it is presently in the pseudocode stage. Intermediate users may use an experiment composer to define a group of pre-compiled SCL segments as forming an experiment. At this stage, the system also requires a specification of the format of the output data stream and the prespecification of any fixed variables for this experiment. An elementary version of the composer is implemented on the IBM. Novice users may access the library of experiments composed in order to execute them using the Run-Time Executive. Each choice is verified against the system configuration file before running to ensure no unspecified hardware accesses. The data structures for both the selector and Run-Time Executive have been defined.

All the data and library files, as well as the data structures used within the suite of programs, have been defined and simulated. All programs within the suite exist at least in functional specification form and mostly in pseudocode form. The suite can be activated from a WIMP shell on the IBM AT, with the analysis program at prototype stage and preliminary versions of the composer and library manager implemented.

REFERENCES

Albrecht, D., DeValois, R. (1981) J. Physiol., 316, 411-414.
Andrews, D.P. (1967) Vision Res., 7, 975-997.
Binford, T. (1981) Artificial Intelligence, 17, 205-244.
Blakemore, C. and Julesz, B. (1971) Science, 171, 286.
Blakemore, C.B., Campbell, F.W. (1969) J. Physiol., 203, 237-260.
Braddick, O., Campbell, F. and Atkinson, J. (1978) In Handbook of Sensory Physiology, Vol VIII, edited Held, R. et al., Springer Verlag.
Brady, J.M., Ponce, J., Yuille, A. and Asada, H. (1985) In Proc. 2nd Int. Symp. on Robotics Research, edited Hanafusa, H. and Inoue, H., MIT Press.
Canny, J. (1983) Finding edges and Lines in Images. MIT AI Lab, Tech. Rep. 720.
Carlson, C., Klopfenstein, R. (1985) JOSA A, 2, 1747-1751.
Cooper, G., Robson, J. (1968) IEE/NPL Conference on Pattern
Recognition. IEE Conference publication, 47, 134-143.
Daugman, J. (1985) JOSA A, 2, 1160-1169.
Derrington, A.M., Krauskopf, J. and Lennie, P. (1984) J. Physiol. 357, 214-265.
Derrington, A., Lennie, P. (1982) J. Physiol., 333, 343-366.
Derrington, A., Lennie, P. (1984) J. Physiol., 357, 219-240.
Derrington, A.M. (1986) Submitted to Vision Research.
DeValois, R.L., Albrecht, D., Thorell, L. (1982) Vision Res., 22, 545-599.
Enroth-Cugell, C., Robson, J. (1966) J. Physiol., 187, 515-572.
Foley, J. (1976) Vision Res. 16, 1263.
Geisler, W. (1984) JOSA A, 1, 775-782.
Graham, N. (1977) Vision Res., 17, 637-652.
Graham, N., Nachmias, J. (1971) Vision Res., 11, 251-259.
Graham, N., Robson, J., Nachmias, J. (1978) Vision Res., 18, 815-825.
Hawken, M.J., Parker, A.J. (1984) Exp. Brain Res., 54, 367-372.
Hawken, M.J., Parker, A.J. (1987) Proc. R. Soc. Lond. Series B, 231, in press
Hendrickson, A., Hunt, S.P., and Wu, J.-Y. (1981) Nature, 292 605-607.
Henning, G.B., Hertz, B.G., Hinton, J. (1981) JOSA, 71, 574-581.
Henning, G.B., Hertz, G., Broadbent, D. (1975) Vision Res., 15, 887-898.
Hildreth, E.C. (1984) The Measurement of Visual Motion. MIT Press.
Horn, B.K.P. (1986) Robot Vision. MIT Press, Cambridge, Mass., USA.
Horton, J.C. and Hubel, D.C. (1981) Nature, 292, 762.
Johnston, E.B. and Parker, A.J. (1987) ARVO abstract.
Julesz, B. and Schumer, R. (1981) Ann. Rev. Psychol. 32, 575.
Julesz, B. (1971) Foundations of Cyclopean Perception, U. of Chicago Press
Kaufman, L., Bacon, J. and Barroso, F. (1973) Vision Res. 13, 137.
Krauskopf, J. and Srebro, R. (1965) Science 150, 1477.
Krauskopf, J., Williams, D.R. and Heeley, D.W. (1982) Vision Res. 22, 1123-1131.
Livingstone, M.S., Hubel, D.H. (1984) J. Neuroscience, 4, 309-339.
Marcelja, S. (1980) JOSA, 70, 1297-1300.
Marr, D. (1976) Phil. Trans. R. Soc. Lond. B, 275, 483-524.
Marr, D. (1982) Vision. W.H. Freeman, San Francisco and Oxford.
Marr, D., Hildreth, E. (1980) Proc. R. Soc. Lond. B, 207, 187-217.
Marr, D., Poggio, T. (1979) Proc. R. Soc. Lond. B, 204, 301-328.
Mayhew, J., Frisby, J. (1981) Artificial Intell., 17, 349-385.
Parker, A., Hawken, M. (1983) Invest. Ophthal. Vis. Sci., 24 (Suppl.), 46.
Parker, A., Hawken, M. (1984) Invest. Ophthal. Vis. Sci., 25 (Suppl.), 314.
Parker, A. and Hawken, M. (1985) J. Opt. Soc. Am. A 2, 1101-1114
Poggio, G., Motter, B., Squatrito, S. and Trotter, Y. (1985) Vision Res. 25 397

Ikeu, ... Ikeu, ...
Richards, W. (...) ... ...
Richards, W. (...) In ... and ... ..., ed. ... ... Harris, pp.177-214,
Erlbaum and Ass. Inc., New York.
Rich ..., ., Spner, ... (...) ... ., ., ... -...
Sadruck, R. (...) Ph.D ... ..., ..., ...
Tikeu, ..., Barlow, H. (...) ... ..., 4., ..-10..
Schumer, R. and ..., L. (...) ... ..., ..., ...
Schumer, R. and Ganz, L. (...) ... ... Am. 64, 187.
Chaurman, K., Dickey, F., ... Brown, J. (...) IEEE Trans PAMI, PAMI-1, 37-49.
Terzopoulos, D. (1984) MIT Ph.D. Thesis.
Tyler, C.W. and Sulesz, B. (197.) ... ... Am. 6., 1365
Tyler, C.W. (197.) Percept ..., 4, ...
Watson, A.B. (198.) In Physical and Biol ... ... Processing of Images, ed.
Braddick, ..., Sleigh, A., pp.... -..., Springer-Verlag, Berlin.
Watson, A.B. and B..., ... (...) ... ..., .., ...
Watson, A.B. et al. (19..) ... ..., ...
Watt, R., Andrews D.l. (19..) ... ..., .., ..-...
Watt, R., Morgan, M.. (19..) ... ..., .., ..-....
Watt, R., Morgan, M.. (19..) ... ..., .., ...-....
Westheimer, G. (1981) Proc. Roy. Soc. ... ..., ., ...
Wiesel, T.N. and Hubel, D.H. (196.) ... ... phy ... ..., ...-115..
Wilson, H.R. (196.) ... ..., ., ...-....
Wilson, H.R., Bergen, J. (19..) ... ..., ...
Witkin, A.P. (1981) Artificial Intelligence, 1., ...-4..
Witkin, A.P. (198.) Proc. 7th Int. ... ... Artif. Intell., Karlsruhe, 1019
Yang, Y. and Parker, A.J. (198.) ... ...
Yuille, A. and Poggio, T. (198.) ... ... Am. A, .., ...-...
Zeki, S. (1980) Nature 284, 41.-41.

APPENDIX: SCIENTIFIC ACTIVITIES OF THE GRANT HOLDERS DURING TENURE OF GRANT
Papers in press and in preparation

Hawken, M.J. and Parker, A.J. (1987) Spatial Properties of Neurons in the Monkey Striate Cortex. Proc. R. Soc. Lond., Series B, 231, in press

Hawken, M.J., Parker, A.J. and Lund, J.S. (1987) Contrast sensitivity and laminar organization of direction selective cells in the striate cortex of Old World monkeys. In preparation.

Parker, A.J. and Hawken, M.J. (1987) Hyperacuity and the Visual Cortex. Nature, in press.

Parker, A.J. and Hawken, M.J. (1987) Detection thresholds and spatial structure of receptive fields in primate striate cortex. To be submitted to special issue of J. Optical Soc. America arising from Rank Prize Symposium (see below).

Conference papers presented and scheduled for presentation

Blakemore, C.B. and Hawken, M.J. (1985) Contrast sensitivity of neurons in the lateral geniculate nucleus of neonatal monkeys. J. Physiol. 369, 37P.

Hawken, M.J. and Parker, A.J. (1986) Laminar distribution of direction selective cells in monkey striate cortex. 6th Winter Conference on Brain Research, 9-15 March, Avoriaz, France.

Parker, A.J. and Hawken, M.J. (1986) Detection thresholds and spatial structure of receptive fields in primate striate cortex. Invited contribution to Rank Prize Funds Symposium on "The Statistical Efficiency of Natural and Artificial Vision.", 16-18 Dec, Cambridge, UK.

Lund, J.S., Hawken, M.J. and Parker, A.J. (1987) Local circuit neuron organization in infragranular layers of monkey striate visual cortex. Accepted by Association for Research in Vision and Ophthalmology (ARVO), Annual Meeting 4-8 May, Sarasota, Florida, USA.

Hawken, M.J., Parker, A.J. and Lund, J.S. (1987) Contrast sensitivity and laminar distribution of direction sensitive neurons in monkey striate cortex. Accepted by Association for Research in Vision and Ophthalmology (ARVO), Annual Meeting 4-8 May, Sarasota, Florida, USA.

Parker, A.J. and Hawken, M.J. (1987) 2-D structure of cortical mechanisms for contrast detection. Accepted by Association for Research in Vision and Ophthalmology (ARVO), Annual Meeting 4-8 May, Sarasota, Florida, USA.

Johnston, E. and Parker, A.J. (1987) Surface curvature as a descriptor of three dimensional shape. Accepted by Association for Research in Vision and Ophthalmology (ARVO), Annual Meeting 4-8 May, Sarasota, Florida, USA.

Yang, Y. and Parker, A.J. (1987) Spatial properties of a disparity pooling process. Accepted by Association for Research in Vision and Ophthalmology (ARVO), Annual Meeting 4-8 May, Sarasota, Florida, USA.

1

SPATIAL PROPERTIES OF NEURONS IN THE MONKEY STRIATE CORTEX

M.J. Hawken and A.J. Parker

University Laboratory of Physiology, Parks Road, Oxford, OX1 3PT, England, UK.

Correspondence to: M.J. Hawken,
University Laboratory of Physiology,
Parks Road,
Oxford, OX1 3PT,
England, UK.

Running title: Receptive field models

With 16 text figures and 2 tables

ABSTRACT

Contrast sensitivity as a function of spatial frequency was determined for 138 neurons in the foveal region of primate striate cortex. The accuracy of three models in describing these functions was assessed by the method of least squares. Models based on difference of Gaussians (DOG) functions were shown to be superior to those based on the Gabor function or the second differential of a Gaussian. In the most general case of the DOG models, each sub-region of a simple cell's receptive field was constructed from a single DOG function.

All the models are compatible with the classical observation that the receptive fields of simple cells are made up of spatially-discrete "on" and "off" regions. Although the DOG-based models have more free parameters, they can account better for the variety of shapes of spatial contrast sensitivity functions observed in cortical cells and, unlike other models, they provide a detailed description of the organization of sub-regions of the receptive field that is consistent with the physiological constraints imposed by earlier stages in the visual pathway. Despite the fact that the DOG-based models have spatially-discrete components, the resulting amplitude spectra in the frequency domain describe complex cells just as well as simple cells. The superiority of the DOG-based models as a primary spatial filter is discussed in relation to popular models of visual processing that use the Gabor function or the second differential of a Gaussian.

INTRODUCTION

A major contribution to our understanding of early visual processing, mainly originating from psychophysical studies in humans, is that the initial stages of the spatial analysis of a visual scene can be considered as a consequence of the operation of a set of spatial bandpass filters on the retinal image (Campbell & Robson 1968; Braddick et al. 1978 for review). A number of models of detection and discrimination judgements in human visual perception have incorporated spatial bandpass filters as crucial components (Wilson & Bergen 1979; Watson 1983; Watt & Morgan 1985). The implementation of procedures for image processing (Marr & Hildreth 1980; Yuille & Poggio 1985) is often based on bandpass mechanisms similar to those proposed in psychophysical models. It is generally thought that the neural mechanisms underlying such a set of bandpass filters are provided by cells in the primary visual cortex(Cooper & Robson 1968; Blakemore & Campbell 1969; Robson 1975; Marr & Hildreth 1980; Sakitt & Barlow 1982; Robson 1983; Watson 1983).

Hubel & Wiesel (1962, 1968) discovered that the majority of neurons in the primary visual cortex of cat and monkey are selectively sensitive to the orientation of edge or bar stimuli and they catagorized them into two main classes: 'simple' and 'complex'. Characteristically, simple cells show discrete sub-regions in their receptive fields (Hubel and Wiesel 1962) and linear spatial summation (Movshon et al. 1978a). Complex cells, on the other hand, do not have spatially separated "on" and "off" regions in their receptive fields (Hubel & Wiesel 1962) and show non-linear spatial summation (Movshon et al. 1978b). Both classes generally exhibit bandpass characteristics as a function of spatial frequency in their responses to drifting gratings and their sensitivity to the contrast of such patterns (Movshon et al. 1978a,b; DeValois et al. 1982) but the linear properties of simple cells would seem to make them better candidates for the spatial filtering of the image (Robson 1975; Marr 1982).

The primary visual cortex receives its principal afferent input from the dorsal lateral geniculate nucleus (LGN), the cells of which have roughly concentrically-arranged receptive fields with spatial antagonism between the centre and the surround (Hubel & Wiesel 1961; Wiesel & Hubel 1966). Hubel and Wiesel (1962) proposed that a cortical simple cell with an even symmetric receptive field could be made up of inputs from a row of geniculate cell receptive fields flanked by rows of inputs from geniculate cell receptive fields of the opposite sign. It seems reasonable to suppose that cortical cells showing linear spatial summation are primarily influenced by neurones also showing linear summation. The major classes of geniculate relay neurones in the primate with this property are linearly-summating 'X-cells' in the parvocellular and the magnocellular layers of the LGN (Blakemore & Vital-Durand 1981; Shapley et al 1981; Derrington & Lennie 1984).

In this paper we attempt to find a suitable model for describing the spatial properties of the receptive fields of neurons in the primary visual cortex. A satisfactory model should allow an accurate estimate of the bandwidth, peak spatial frequency, cut-off spatial frequency and peak sensitivity of the neuron's spatial contrast sensitivity function, as well as reflecting the structural organization of the receptive field as conventionally plotted. We needed such an accurate model of cortical receptive fields to allow us to compare the contrast thresholds of single neurons with those determined psychophysically for human observers (Parker & Hawken in preparation). Initially, we chose the Gabor function to provide a smooth fit to the spatial contrast sensitivity functions of cortical neurons because it had been used successfully to describe the spatial frequency tuning functions of neurons in the cat's visual cortex (Marcelja 1980; Kulikowski & Bishop 1981; Kulikowski et al.

1982) while also being the basis for some models of visual processing (Sakitt & Barlow 1982; Watson 1983; Daugman 1984). However the Gabor model produced generally inaccurate estimates of the shape of the sensitivity function, most notably the height and location of the peak of the fitted function usually differ from those of the data. We also tried functions based around the second differential of a Gaussian, which have been used extensively in computer vision programs that find edges in images (Marr & Hildreth 1980). The imperfections of these two models led us to the quantitative formulation of a different model, based on the likely organization of the physiological inputs to the visual cortex, which was qualitatively outlined by Hubel and Wiesel (1962). Here we show that this scheme, which is physiologically plausible but requires many parameters, gives much better fits to the spatial contrast sensitivity functions than mathematically simpler functions, derived from computational analyses of visual processing, such as the Gabor or second differential of a Gaussian. Next we describe the new model, as well as the others, in detail.

MODELS

For simple cells, which show linear spatial summation, the spatial contrast sensitivity function will be the amplitude portion of a Fourier representation of the receptive field profile. The shapes of the spatial frequency tuning function and the spatial weighting function are thus directly related (Movshon et al. 1978a; Andrews & Pollen 1979; Dean & Tolhurst 1983), although phase information is required for a complete representation (e.g. Enroth-Cugell et al. 1983). In fact any well-specified model of the receptive field profile must make some prediction of the characteristic shape of the spatial contrast sensitivity function. Even for non-linear complex cells, at least in the cat, the inverse transform of the spatial frequency tuning function relates quite accurately to the 'sub-unit' structure of the overall receptive field determined by measurements of local summation within the field (Movshon et al. 1978b) and may provide an accurate measure of the spatial filtering of the receptive field, even though the output is highly non-linear.

In 1966 Enroth-Cugell and Robson showed that the spatial contrast sensitivity function of X-cells in the cat's retina could be well described by the difference of two Gaussian weighting functions, a model that was proposed initially by Rodieck (1965). This approach, relating the space and spatial frequency domains, has been widely used in quantitative analyses of visual processing. The difference of Gaussians function, as usually applied to retinal ganglion cells and lateral geniculate neurones, is a rotationally symmetrical function with a single spatial variable, the distance r from the receptive field centre, although deviations from rotational symmetry have been noted (Levick & Thibos 1980; Dawis et al. 1984; Soodak 1986).

Many cortical neurons have receptive fields that are elongated in the central excitatory region (correlating with their selectivity for orientation), thus forfeiting the condition of rotational symmetry. But in the direction orthogonal to the elongated axis or preferred orientation, the receptive fields of simple cells have spatially segregated sub-regions of opposite sign. This is the sub-structure giving them their bandpass characteristics in spatial frequency. The individual sub-units of complex cells may have similar properties (Movshon et al. 1978b; Spitzer & Hochstein 1985a,b). Therefore by constraining the comparison of cells and models to the dimension orthogonal to the preferred orientation, the bandpass nature of the cell's receptive field can be investigated.

Figure 1 illustrates the general form of some hypothetical spatial weighting functions, in the direction orthogonal to the preferred orientation, of receptive fields with even symmetry (figure 1b), intermediate symmetry (figure 1c) and odd symmetry (figure 1d). These all have the same bandpass spatial contrast sensitivity functions (figure 1a) in the frequency domain. All realistic models must allow the receptive fields of cells to attain the general shapes of either pure even symmetric, pure odd symmetric or somewhere between the two, as shown in figure 1 (Kulikowski & Bishop 1981). The rest of this section is devoted to describing, in detail, the models that are evaluated in this paper.

Text figure 1 near here

Models based on difference of Gaussians (DOG) functions

The first model treats each sub-region of a simple cell's receptive field as if it were derived from a single lateral geniculate neuron with a difference of Gaussians (DOG) profile for its receptive field (Rodieck 1965; Enroth-Cugell & Robson 1966; Derrington & Lennie 1984). Consider, for example, a hypothetical simple cell receptive field with a discrete central "on" sub-region and two flanking "off" sub-regions, equally spaced either side of the central region. Such a conventional "hand-plotted" receptive field is shown in figure 2a.

Text figure 2 near here

The underlying sensitivity profile of the "on" region in the hand-plot is itself a DOG (the weighting function of an on-centre LGN cell giving excitatory input to this simple cell), whose centre component responds to an increment in brightness and whose surround component is of opposite sign. The flanking "off" sub-regions of the hand-plot are also each a DOG, but of opposite configuration to that comprising the "on" sub-region (e.g. the weighting functions of off-centre LGN cells). The peaks of the Gaussians forming the flanking "off" sub-regions are spatially separated from ones forming the central "on" sub-region. The second row in figure 2a gives the spatial profile of each of the separate Gaussians, which make up the receptive field shown in the third row of figure 2a. An alternative form of this model may have just two sub-regions, corresponding to an odd symmetric receptive field, as illustrated in figure 2b.   A receptive field intermediate between pure even and pure odd symmetry, with unbalanced flanking regions, can also be created with this model, by varying the relative amplitudes of the flanking DOGs.

Each component Gaussian in this model must be specified by three parameters: the peak amplitude, spatial location of the peak amplitude and the space constant of the Gaussian. It is mathematically convenient to place the origin of the spatial co-ordinate system at the location of the peak of the central sub-region. This sub-region can therefore be specified by 4 parameters: the space constants of the Gaussians (x_c and x_s) and their amplitudes (k_c and k_s). In general, a flanking sub-region must be specified by five parameters, four of which are equivalent to those describing the centre subregion (x_{c_2} , x_{s_2} , k_{c_2} , k_{s_2}) and a fifth, which is the separation (S) of the peak of 2 the2 flanking sub-region from the peak of the centre sub-region. Thus nine parameters would be sufficient to describe an odd-symmetric receptive field composed of two sub-regions as shown in figure 2b.

Rather than adding a further set of 5 parameters to describe a receptive field with 3 sub-regions as in figure 2a, we constrained the model so that both flanking sub-regions had the same spatial properties. With this constraint, the introduction of a symmetry parameter (g) allows a description of the full range of behaviour from pure even symmetry to pure odd symmetry as illustrated in figure 1. When g is 0.0, the model has only one flanking sub-region. When g is 0.5, the model depicts a receptive field with two identical flanking sub-regions. When g is 0.25, there are two flanking sub-regions with identical space constants, but the amplitude of one is greater than the other in a ratio of 2:1.

For a purely bandpass spatial contrast sensitivity function, with no reponse at all below a certain low spatial frequency, the sensitivity of the central sub-region $(k_c - k_s)$ minus the sensitivity of the flanking sub-regions $(k_c 1 - k_s 1)$ should be zero (i.e. the centre and the flanks of the receptive field should be balanced). On the other hand, for a bandpass spatial contrast sensitivity function with a significant lowpass component, $(k_c - k_s)$ will be greater than $(k_c - k_s)$. Because most neurons show bandpass spatial contrast sensitivity functions, without a large lowpass component, we imposed a final constraint on this model such that the combined sensitivity of all sub-regions summed to zero. This means that the receptive field should give zero response to changes in the overall illumination level. This has the advantage of reducing the number of free parameters in the model from ten to nine (see appendix: equation 1). For a cell with a significant lowpass component in the spatial contrast sensitivity function, the model obviously should not be constrained in this manner.

We have called this model, with nine parameters, d-DOG-s (the difference of the difference of Gaussians with separation). Although the choice of parameters almost certainly under-represents the actual one-dimensional organization of the receptive field, even this large number of parameters makes the model complicated and difficult to test. Fortunately, the d-DOG-s model can be well approximated by functions that are subsets of this model and have a reduced number of parameters: ---
(i) The simple DOG model. In this case the cortical receptive field is modelled with a single DOG function, specified by four parameters: the space constant (x_c) and amplitude (k_c) of the centre Gaussian and the space constant (x_s) and amplitude (k_s) of the surround Gaussian, where the peaks of the centre and surround space constants are spatially co-incident (see appendix: equation 3). In this simplified model, the flanking sub-regions of the receptive field are formed by the extremities of the surround Gaussian because of the difference in spatial extent of the centre and surround components. This is the minimal version of the d-DOG-s model that retains the spatial bandpass characteristic required to model cortical cells. It is also easy to compare quantitatively with the Gabor model because they both have four parameters (see figure 14). The DOG has been proposed previously as the basis of a model of cortical neurons (Rose 1979). An example of the hand-plotted receptive field, the component Gaussians and the resultant spatial weighting function of the difference of two Gaussians is illustrated in figure 3a. In the form used here, this model is always of even symmetric form.

Text figure 3 near here

(ii) The DOG-s model. In order to test the importance of the parameter (S) that specifies the separation of the peaks of the centre and flanking sub-regions of the receptive field, we stripped as many parameters as possible from the d-DOG-s model whilst retaining the characteristic behaviour associated with the separation parameter. This resulted in the DOG-s model, which is the even symmetric form of the d-DOG-s model with only the centre components of the DOGs $(x_{c_1}, k_{c_1}, x_{c_2},$

k_{c_2}) and the separation parameter (S) retained (see appendix: equation 2).
Figure 3b shows that this leaves 3 Gaussian mechanisms, where each sub-region of the receptive field is served by a single Gaussian. The two Gaussians specifying the flanking sub-regions were constrained to have the same space constants and sensitivity parameters. This constraint is similar to that applied to the d-DOG-s model. To the extent that the surrounds of LGN neurons are weak, particularly in the parvocellular layers, the DOG-s model (which simply lacks the components due to these LGN surrounds) retains the significant features of the general case.

This function reduces to the simple DOG when the separation parameter is zero. Indeed the DOG-s model can be considered as a rearranged version of the DOG model, where the surround has been split into two Gaussians and the peaks of the two halves have been relocated at distances $+S$ and $-S$ from the peak of the centre mechanism (figure 3b). For this reason, the notation of the DOG model has been followed in describing the DOG-s model and the parameters of the flanking regions are therefore designated by k_s for sensitivity and x_s for the space constant. On the other hand, in terms of the d-DOG-s model, these parameters associated with the flanking sub-regions would be k_{c_2} and x_{c_2}.

The sub-units of the DOG models can most easily be considered as derived from individual geniculate cells with a centre/surround receptive field organization. In order to preserve the relationship between the values of the space constants and amplitudes of the centre and surround mechanisms of LGN neurons and those obtained from the fitting of DOG models to the cortical data, bounds were imposed on the parameters during the fitting procedure. Thus the peak contrast sensitivity and space constant of the centre mechanism were constrained to be within the bounds of values found for geniculate neurons (Kaplan & Shalpey 1982; Derrington & Lennie 1984). Most often the choice of parameter values to give the best-fitting function did not reach the bounding constraints because the selected values fell naturally in the range found for geniculate cells. Of course, the imposition of constraints on a parameter puts the constrained version of a model at a disadvantage with respect to the unconstrained version. However, in the case of the DOG-based models, this disadvantage is outweighed by the fact that the parameter values can be given a direct functional interpretation (see Discussion).

The Gabor Model

The Gabor function has been proposed as a model for the receptive field profiles of simple cells (Marcelja 1980; Kulikowski et al. 1982; Daugman 1985; Field & Tolhurst 1986), and for psychophysically-defined channels (Watson 1983; Daugman 1984). If one wishes to represent an image in terms of space and spatial frequency, the Gabor representation is optimal in terms of compactness, minimizing the uncertainty associated with localizing a signal simultaneously in space and spatial frequency. This fact has been considered to be of potential significance for the efficient processing of visual information (Marcelja 1980; Daugman 1984, 1985). The function is the product of a sinusoid with a single Gaussian envelope (see appendix: equation 4) and is defined by four parameters: the space constant of the Gaussian (x_c) and its amplitude (k_c), the frequency of the sinusoid (f_c) and the phase of the sinusoid (p) with respect to the Gaussian. Spatial weighting profiles given by this function, for two cells, are shown in figure 9a,b and can be seen to have roughly the shape required for the hypothetical spatial weighting of a bandpass filter shown in figure 1.

The Differential of a Gaussian Model

The Laplacian of a Gaussian ($\nabla^2 G$) was introduced by Marr & Hildreth (1980) as a model of the concentrically organized receptive fields of retinal ganglion cells, to support a representation of the image based on zero-crossings. We have considered a one-dimensional version of this, the second differential of a Gaussian ($D^2 G$), as a model of cortical cells. This function has two parameters, the space constant of the Gaussian (x_c) and a scaling constant (k_c) (see appendix: equation 5). Figure 10a,b illustrates two examples of the spatial weighting profile. A particular constraint imposed by this function is that the low frequency portion of the predicted spatial frequency tuning function is a straight line with a slope of two in logarithmic co-ordinates. Marr & Hildreth (1980) pointed out that the Laplacian of a Gaussian can be approximated by a circularly symmetric DOG function, provided that the ratio of the surround space constant to the centre space constant is 1.6:1 or smaller. Such a relationship would also clearly be true for the $D^2 G$ model and the DOG model discussed earlier. It is important to appreciate that the DOG function is equivalent to $D^2 G$ only if this constraint applies. In the results presented here applying this constraint would result in the mistaken conclusion that the DOG model is a poor description of the spatial contrast sensitivity functions because the ratio of surround to centre space constants is seldom less than two.

We have also considered a model comprised of two $D^2 G$ functions of opposite sign, spatially separated by $2x_c$, since this function has been given prominence as a specific model for simple cells in computational theories of vision (Marr & Hildreth 1980; Marr & Ullman 1981; Marr 1982). This model, however, produced even less satisfactory fits to the spatial contrast sensitivity functions than the $D^2 G$ function, so the detailed results have not been included.

METHODS

Physiological experiments were performed on 8 adult Old-World monkeys (7 *Macaca fascicularis* and 1 *Cercopithicus aethiops*) weighing between 3.3 and 5.5 Kg.

Preparation

Animals were anaesthetized with i.m. Ketamine for venous cannulation and then maintained on i.v. steroid anaesthetic (Saffan) for the ensuing surgery. All incisions were infiltrated with long-lasting local anaesthetic (Marcain) and any pressure points were treated with topical anaesthetic (Tronothane). For recording, animals were anaesthetized with barbiturate (Sagatal; 6 mg kg^{-1}), and paralysed with pancuronium bromide (Pavulon; 0.2 mg kg^{-1}); then both the anaesthetic (Sagatal; 1.2 - 3.0 mg kg^{-1} hr^{-1}) and muscle relaxant (Pavulon; 0.2 mg kg^{-1} hr^{-1}) were continuously infused intravenously, in a solution of 10% glucose in 0.9% NaCl at 5.6 ml hr^{-1}, to maintain anaesthesia and paralysis. The electrocardiogram (e.k.g) and electroencephalogram (e.e.g) were monitored continuously and the anaesthetic state was judged to be satisfactory if there was almost continuous slow-wave e.e.g. activity and if mildly noxious stimuli produced no change in e.e.g or heart rate. Supplementary anaesthetic doses were administered, if necessary, to maintain the anaesthetic state. Animals were artificially hyperventilated with room air to which CO_2 was added to maintain end-expiratory CO_2 at 4.5 - 5.5%. Rectal temperature was monitored continuously and maintained at 37.5 - 38 °C.

The pupils were dilated by topical application of atropine sulphate and zero-power contact lenses were fitted to protect each cornea. The animal viewed the

visual display through 3 mm artifical pupils and additional spherical correcting lenses. The refractive state of each eye was initially judged by direct ophthalmoscopy and further checked at intervals throughout the experiment by determining the highest spatial frequency that evoked a response just greater than the background firing of a neuron and adjusting the lenses if necessary.

Recording

Glass-coated tungsten micro-electrodes (Merrill & Ainsworth 1972) with 4-8 μm exposed tips were lowered to the cortical surface, through a small craniotomy and durotomy, under visual control and the exposure was sealed with 2% agar in 0.9% saline. The whole area was covered with a mixture of paraffin oil and vaseline to prevent drying. Action potentials were amplified and the individual spikes of well-isolated neurons selected by a level discriminator that triggered a standard TTL pulse as output to a computer. Successive traces of the recording were superimposed on a storage oscilloscope triggered by the level discriminator, to allow monitoring of the waveform of the action potential and to assess whether the recording was from a single cell.

Visual stimuli

Receptive fields were plotted by hand with lines, bars or spots back-projected on a tangent screen 171 cm from the animal. The projections of the foveae were marked on the tangent screen by using an ophthalmoscope with a reversing prism (Eldridge 1979); repeated determinations of the projection of the same retinal position were always within 0.5 deg. and most often 0.25 deg. or less. From the hand plots of receptive fields we determined the eccentricity, an initial classification of cell type (simple or complex), the ocular dominance (Hubel & Wiesel, 1962) and some indication of the colour preference using broad-band Wratten filters. The simple/complex categorization was further analysed, quantitatively, using a test of linearity of spatial summation. For quantitative assessment of responses to visual stimuli, gratings varying sinusoidally in luminance profile were displayed on a cathode-ray tube (Joyce Electronics), 30cm x 22cm with a white (P4) phosphor (luminance: 280 cd m^{-2}), positioned 342 or 456 cm in front of the animal. The bars of the grating could be restricted in height, to produce a strip of grating flanked by uniform areas of the same mean luminance, so as to optimize the stimulation conditions for cells with end-stopped receptive fields (Hubel & Wiesel 1965; Bishop et al. 1971; Gilbert 1977), for which elongated bars were relatively ineffective.

Measurement of response properties

Spatial frequency response tuning.

The magnitude of the response to a range of spatial frequencies presented in pseudo-random order at a contrast of 0.7 was measured for between 10 and 20 presentations of each stimulus sequence, consisting of at least 2 cycles of a drifting grating. The orientation, drift rate and direction of motion were optimized by listening to the responses before the tuning function was determined.

Orientation tuning.

The response of the unit was determined at a number of orientations for both directions of drift, the steps in orientation varied between 2.5° for the most sharply tuned cells and 20° for cells with little or no preference for orientation. The spatial frequency of the grating used was that which gave the largest response

during measurement of spatial frequency tuning and the contrast was always 0.7. Each stimulus was presented between 5 and 20 times in pseudo-random order.

Spatial summation.

The response to stationary, contrast modulated gratings was determined at 12 phase angles, covering 360° (the dimension of one full cycle of the grating) in 30° steps. Each phase was presented for 2 temporal cycles, the contrast being modulated sinusoidally between zero and 0.7 at the optimal temporal frequency for the cell. Each stimulus was presented 10-20 times with all phases selected in a pseudo-random order. During the analysis of data after the experiment, we determined the spatial frequency at the peak of the response function. Because there are some cortical cells that appear to be predominantly linear at low spatial frequencies but non-linear at high spatial frequencies (Movshon et al. 1978 a,b), only those cells for which the spatial frequency of the test grating on the summation test was 0.7 times the peak spatial frequency or greater are included here.

Contrast sensitivity

To determine the contrast sensitivity of neurons, we used a staircase method similar to that described by Derrington and Lennie (1982). For gratings of various spatial frequencies covering the range over which the cell responded (determined from the spatial frequency response tuning) we measured the contrast sensitivity of the cell using this staircase method. Initially, the mean and the variance of the background discharge of the cell were determined, with the receptive field of the cell centred on the display with no grating present. The mean was calculated over 16 periods, each period equal in duration to the period for which the grating stimulus would be presented. Then a drifting grating was presented (without change in mean luminance) and the spikes elicited during the presentation were accumulated, discounting the duration corresponding to the first half cycle of the grating to avoid temporal transients. Following this there was a pause, equal to the presentation time of the grating, then a further period during which another single measurement of the background firing was made, before the next grating was displayed. An on-line running estimate of the mean and variance of the background was determined using the values collected in the 16 most recent periods of measurement. Following the presentation of each stimulus, the number of spikes occurring during that particular trial was compared with a statistical criterion (two standard deviations greater than the background mean for these experiments). If the evoked response exceeded the criterion, the contrast was reduced on the next trial at that particular spatial frequency; if not, the contrast was increased. The staircase was run at each spatial frequency until the computer had accumulated at least 8 reversals (in later experiments, 24 reversals) at a step size of 0.0125 log unit, or until there was no response greater than the criterion at the highest possible contrast (0.7). The order of presentation of spatial frequency was chosen randomly by the computer. Using this method, we could obtain a complete spatial contrast sensitivity function for each cell at its optimal orientation. This took between 15 and 45 minutes, depending on the number of spatial frequencies, the rate of convergence of the staircase and the other stimulus parameters.

For all measures, other than the staircase determination of contrast sensitivity, the computer accumulated on-line peri-stimulus time histograms (p.s.t.h's) for each stimulus condition and for a blank period. In addition the total number of spikes elicited on each stimulus presentation was stored along with an estimate of the magnitude of the fundamental component of the response, at the temporal frequency of the drifting grating (Derrington & Lennie 1982).

Histology

The position of the tip of the electrode was marked at regular intervals by making small electrolytic lesions (2-3 μA for 2-3 s, tip negative). At the end of the experiment the animal was killed with an overdose of anaesthetic.   The methods used in perfusion, histological reconstruction of penetrations and assignment of laminar position for each cell has been described previously (Hawken & Parker 1984).

RESULTS

Cell classification

Some cells could be clearly classified as simple: the hand plot of their receptive fields revealed spatially segregated "on" and "off" sub-regions that were mutually opponent; on the test of spatial summation, they produced modulated responses in phase with the temporal modulation of the stimulus at some spatial phases, while showing clear null positions (no response despite modulation of the grating) at π/2 radians from the phase that gave the biggest response; with drifting sinewave gratings, the responses at all spatial frequencies were strongly modulated at the temporal frequency of the stimulus.

Other cells showed all the characteristics of classical complex cells: they gave "on/off" responses at all positions in their receptive fields to a flashing bar; they produced a clear second harmonic response at all spatial phases on the test of linearity of spatial summation; with drifting gratings, they showed little or no response modulation at the temporal frequency of the stimulus but responded with an increase in the mean discharge. However, there were cells that did not fall clearly into either of these categories. For example, some cells which in most respects appeared simple, gave an indication of a second harmonic response at the expected null position, especially for spatial frequencies on the high frequency limb of the spatial frequency tuning function.   But these cells showed modulated responses to drifting grating stimuli. Although some of the anomalies could be attributed to slow drifts of the eyes or pulsations due to cardiovascular or respiratory movements, experience in the cat, where the receptive fields are larger and these mechanical problems not so severe, suggests that there are cells that genuinely show a mixture of linear and non-linear behaviour at many spatial frequencies.

To obtain a quantitative indication of the degree of linearity of spatial summation, the response of each cell was determined, for a set of spatial phases covering covering the full 2π radians of phase angle in steps of π/6 radians.   The details of the test are presented in the METHODS section.   For retinal ganglion cells and for lateral geniculate neurons, the ratio of the mean of the second harmonic responses (f2) to the peak amplitude of the fundamental response (f1) has been used as an index of linearity of spatial summmation (Hochstein & Shapley 1976; Derrington & Lennie 1984).

Text figure 4 near here

Figure 4 shows that the distribution of f2/f1 ratios is weakly bimodal   for   the total sample of cortical cells (cf. Dean & Tolhurst 1983). DeValois et al (1982) used the ratio of the fundamental to DC response (f1/f0) for drifting gratings to classify cells in the macaque striate cortex. They found a more clearly bimodal distribution of the f1/f0 ratio and distinguished their population on the basis of

this test. In this paper, simple cells have been classified as those with a f2/fl ratio less than one for stationary modulated gratings, which indicates that the fundamental component dominates over the second harmonic. Complex cells have been classified as those with f2/fl ratios of greater than one, which indicates a dominant non-linear component. Based on the f2/fl index, we have 77 simple and 61 complex cells. These percentages of simple and complex cells based on the f2/fl index are very similar to those found by DeValois et al. (1982), which is to be expected since both the tests define simple cells as those having a prominent fl component.

Measurements of contrast sensitivity

For each cell, the measurement of contrast sensitivity was obtained at spatial frequencies of about one third of an octave apart, using the staircase procedure described in the METHODS. In order to determine the correct transformation of the data to use in fitting the curves to the data by the method of least squares, the relationship between the mean and variance of the contrast sensitivity measurements was investigated. In three of the eight animals, we collected 24 reversals (rather than the normal 8) on the staircase measure of contrast sensitivity. This gives 12 independent measures of threshold at each spatial frequency and from these the variance of the mean contrast threshold was estimated (Wetherill & Levitt 1965). There is a clear positive relationship between the arithmetic mean and variance of linear contrast values (variance $= k*mean_1{}^{1.85}$; see figure 5). Because the exponent of the power function relating the mean and variance was almost two, a logarithmic tranformation of the contrast sensitivity values was taken to make the data homoscedastic. For models specified in equations 1,2,3 and 4 a general purpose minimization routine was used (STEPIT: Chandler, J.P.) to find the best-fitting functions, whereas a logarithmic transformation makes equation 5 linear, so for this model the best fit was obtained by direct solution of the normal equation.

Text figure 5 near here

Evaluation of models

In each figure that shows contrast sensitivity as a function of spatial frequency (e.g. figure 6) the mean contrast sensitivity at each spatial frequency is shown by the open circles ($\pm$ one SD). The contrast sensitivity measurements obtained for two simple cells are shown in the left panels of figures 6-10, with the smooth curves being the best-fitting versions of the amplitude spectra of the models: d-DOG-s (figure 6a,b), DOG-s (figure 7a,b), DOG (figure 8a,b), Gabor (figures 9a,b) and D^2G (figure 10a,b). The two examples were chosen because they 1) had relatively high sensitivities (allowing the models to be discriminated from one another), 2) had intermediate bandwidths for our sample of cells, 3) came from different laminae in the region of the cortex devoted to foveal vision and 4) showed relatively low variance over the data points (again allowing the models to be most readily discriminated). Figure 13 shows a wider variety of sensitivity functions, including some of the most extreme forms. The two examples are shown in each of the five figures (6-10). The right panel shows the spatial weighting function associated with the sensitivity function shown in the corresponding left panel.

Text figures 6,7 and 8 near here

For each model the parameters were chosen so that they minimized
$$\sum (\log(model) - \log(data))^2$$
In order to provide an estimate of the deviation between the measured values of contrast sensitivity and the best fitting function from each model, the above quantity was divided by the number of data points to give the mean error per data point (Linsenmeier et al. 1982). The mean error allows a comparison between cells with different numbers of values making up the spatial contrast sensitivity function. For the cell whose sensitivity function is illustrated in the top of figures 6-10, the mean error for the best fitting version of each model is given in table 1a, while the error associated with each model for the cell illustrated in the lower half of figures 6-10 is given in table 1b.

Text figures 9 and 10 and table 1 near here

Both on visual inspection of the fits to the spatial contrast sensitivity functions and in terms of the mean error per data point, models based on the difference of Gaussians provide a much more accurate description of the spatial tuning than do the Gabor or the second differential of a Gaussian. An F-test for lack of fit of a model, using the standard procedures for linear regression, can be obtained by comparing the estimates of variance measured during the experiment with the residual sum squares deviation of the fitted function from the data. Unfortunately, this procedure is only exactly valid for models that can be made linear in their parameters, such as D^2G. It is not well established that the other four models can be treated in this way, because they are nonlinear in their parameters. Nonetheless, although the exact values of F-ratios should be interpreted conservatively, they do provide a useful measure of comparative performance (Draper and Smith 1966, page 282, page 299). With the number of degrees of freedom for the data in table 1, even F-ratios as small as 6 would be associated with a significance level of < 0.001. All the firm conclusions we wish to draw concerning these models are supported by F-ratios of 60 or greater.

The results of the F-ratio test are clear for D^2G, which is linear in its parameters: both cells in figure 10 show significant lack of fit (see table 1). The values of the F-ratio for the Gabor model (figure 9) are also very large. Thus, both these models can be confidently rejected.

Two aspects of the inability of the Gabor and D^2G functions to match the shape demanded by the data points in figures 9 and 10 are particularly striking. First, the low frequency limb of the tuning curve is poorly described. Second, a consequence of the attempt by the fitting procedure to accommodate the low frequency limb is that the peak spatial frequency of the model functions is far removed from the peak defined by the data (half to one octave too high). The attempt to fit the low frequency limb of the tuning curve also explains why the fitting procedure arrived at a purely odd symmetric version of the Gabor function. Any purely odd symmetric receptive field necessarily has zero response at zero spatial frequency. Hence selection of the odd-symmetric version of the model by the fitting procedure allows the steepest possible low frequency roll-off in the amplitude spectrum, but even this choice is inadequate.

The DOG-s and DOG models differ only in the inclusion of a separation parameter (S) for the DOG-s model. This parameter is an additional complication but has some

particularly attractive interpretations in terms of receptive field organization and its possible anatomical substrate (see Discussion), so it is important to assess quantitatively the case for its inclusion. A partial F-test (Draper and Smith 1966, pages 67-72) can be applied to examine whether a particular parameter significantly improves the fit of a model. The F-ratio is again very large: $F(1,134) = 74.8$ for the cell in the upper half of figures 6-10, $F(1,124) = 74.1$ for the cell in the lower half of figures 6-10. These results argue strongly for the inclusion of the separation parameter.

Spatial weighting functions

Each model and its parameters have associated with them a characteristic spatial weighting function. Since the spatial contrast sensitivity measurements that define the amplitude spectra place quite strong constraints on the shape of the best-fitting function and the parameter values associated with the function, it is informative to compare the shapes of the spatial weighting functions derived from each of the models. The right hand columns in figures 6-10 show the associated spatial weighting functions for each of the amplitude spectra in the left-hand column. Although these weighting functions were not derived from independent experimental measures, the difference in their shapes illustrates how the choice of a DOG-based model as opposed to a Gabor function or second differential of a Gaussian would result in different predictions for the spatial organization of the receptive field.

A second important feature of the spatial weighting functions is that they show that some parameters of the receptive field are robustly defined. The space constants of the centre Gaussian mechanisms for the three DOG-based models applied to the contrast sensitivity function of the cell, shown in the upper half of figures 6-8, are almost identical (2.22, 2.21, 2.38 min arc for d-DOG-s, DOG-s and DOG respectively), while a similar close correspondence holds for the cell in the lower half of each of these figures (2.23, 2.19, 2.45 min arc). In the case of DOG-s, which we have argued is a very reasonable approximation to d-DOG-s, those parameters that are common to both models have values that are within 20%, for the two cells in figures 6 and 7. The DOG-based models also allow realistic comparisons to be made between cells in the striate cortex and those in the lateral geniculate nucleus. In general, the sensitivities and space constants of the centre mechanisms of cortical cells derived from the DOG-based models fall very nicely in the range of values found for the centre mechanisms of neurons in the LGN (Derrington & Lennie 1984).

Comparison between models for the entire sample of neurons

Figure 11 shows the mean error per data point plotted against the variance per data point, also calculated on logarithmically transformed contrast values. Each panel shows the analysis of one of the models, with simple cells indicated by open symbols and complex cells by filled symbols. The diagonal line on each graph is where mean error per data point is equal to variance per data point. For points above this line, error is greater than the variance. The points for the d-DOG-s model are distributed roughly evenly around the diagonal line (figure 11a), while the remaining graphs (figure 11b-e) have been arranged in order of increasingly poor fits of the models to the data points. Data from simple cells and complex cells are similarly distributed throughout each plot. Hence, neither the variance of contrast sensitivity measurements, nor the error associated with the fit of any of the functions, would help to distinguish these two groups of cells. The order of quality of fit, from best to worst, indicated by figure 11 b-e is DOG-s, DOG, Gabor and D^2G. Thus, for the whole sample of cells studied, the DOG-based models (figure 11a-c) provide a better description of spatial contrast sensitivity functions than

the Gabor function (figure 11d) or the second differential of a Gaussian (figure 11e).

Although there are a few relatively large errors, greater than 0.02, for the sensitivity data fitted by the d-DOG-s model, these are almost invariably due to single individual data points that are far removed from the fitted curve. Whether these are truly characteristic of the particular spatial contrast sensitivity function or whether they represent statistical outliers could be decided only by making repeated measurements on the same cell.

<div align="center">Text figure 11 near here</div>

The distribution of error with respect to variance gives a good overall picture of the abilities of each model to describe the spatial contrast sensitivity function, but it does not show whether there is an exclusive subset of cells for which a single model provides the optimal description, even though that model might be inappropriate for the majority of cells. To examine whether there was any clustering of neurons on the basis of the quality of fit, the errors associated with the application of two models were compared. Figure 12 shows the results of this comparison for each cell for the DOG-s, DOG, Gabor and D^2G (figure 12 a,b,c,d respectively) plotted against the d-DOG-s model. It can be seen that the d-DOG-s model fits the contrast sensitivity measurements of all cells at least as well as or better than any of the other models.

<div align="center">Text figure 12 near here</div>

Further examples of spatial contrast sensitivity functions that are well described by the d-DOG-s model are shown in the upper six panels of figure 13. These illustrate the wide variety of shapes found for cortical cells and the flexibility of the d-DOG-s model in accounting for them. The values of the parameters for the best-fitting version of the d-DOG-s model are shown in table 2. The lowest two panels show examples of cells for which the simple DOG model (figure 13g) or indeed a single Gaussian (figure 13h) are adequate to describe the data. The sensitivity function shown in figure 13b is one of the most narrowly tuned that we have encountered; as can be seen, its sensitivity function is well described by the d-DOG-s model and the associated spatial weighting function would have multiple antagonistic zones (Kulikowski & Bishop 1981; Kulikowski et al. 1982).

<div align="center">Text figure 13 & table 2 near here</div>

It is obviously to be expected that the d-DOG-s model will be as good as or better than the DOG-s and DOG functions, because elimination of some of the parameters from the d-DOG-s model produces the equations of DOG-s and DOG (i.e. DOG-s and DOG are straightforward reductions of d-DOG-s). Comparisons between d-DOG-s and the Gabor model (figure 12c) and d-DOG-s and the second differential of a Gaussian (figure 12d), indicates that there are no cells for which the Gabor or D^2G models provide a better description of the data than d-DOG-s. Of course, it should be remembered that the number of free parameters in the d-DOG-s model is greater than both the Gabor and D^2G. However, both the DOG function and the Gabor function, as implemented, have four free parameters and therefore a simple comparison between them is justified.

Text figure 14 near here

In figure 14d we have explicitly compared these two models. The mean error associated with the best-fitting Gabor is plotted on the abscissa while the error for the DOG is shown on the ordinate. Cells whose sensitivity functions were equally well fitted by either the Gabor or the DOG would lie on the solid diagonal. Points below this line signify that the DOG produces a better fit than the Gabor, while those above the line favour the Gabor fit. While the DOG model provides a better description of the majority of cells, there are some for which the Gabor function has a lower error than the simple DOG. For the neuron illustrated in figure 14, the Gabor function (figure 14a) fits the measured contrast sensitivity values very well, having mean error of 0.0028. For comparison, the DOG fit (shown in figure 14b) has a mean error of 0.0131, about five times greater than that of the Gabor. This is, in fact, the largest difference in favour of the Gabor of all the cells that we have tested. However, the DOG-s model (figure 14c) has a slightly lower error than the Gabor. Again, the addition of the separation parameter to the basic DOG model considerably improves the fit.

DISCUSSION

It is clear that, of the models considered in this paper, the d-DOG-s model can account most accurately for the spatial contrast sensitivity functions of cortical neurons. Therefore, in spite of the its many parameters, the d-DOG-s can be considered as preferable for the determination of characteristics of tuning functions, such as bandwidth, peak spatial frequency, peak sensitivity and acuity, that are often quoted in comparison with those derived from psychophysical studies or in computational theories of early visual processing. For many cells, the reduced DOG-based models provide fits that are indistinguishable from the d-DOG-s model (figure 12a,b) and therefore provide simpler yet adequate descriptions of the spatial tuning. For a few cells, the Gabor function gives excellent fits to their spatial contrast sensitivity functions (e.g. figure 14a), but over the whole sample of cells it is poorer than the DOG-based models (figures 12c,14d). D^2G is just poor overall (figures 11e,12d).

It is probably not surprising, that the few explicit models of cortical receptive field structure previously considered, based on the the Gabor (Marcelja 1980), the DOG (Rose 1979) or on a restricted version of the d-DOG-s (Heggelund 1981; Soodak 1986) have all been deemed to be adequate, because they do, qualitatively, attain the general shape of a bandpass device. It is only when quantitative measures from a large sample of cortical neurons are examined comparatively that the differences between the various models become evident.

Receptive field organization

Comparison of DOG-based models

Although the d-DOG-s and DOG-s models give better overall fits to the spatial contrast sensitivity functions than the simple DOG, their improved performance is at the expense of the introduction of extra free parameters, most significantly the separation parameter (S) that distinguishes the DOG-s and DOG models. However, it is possible to give an appealing functional interpretation of the separation parameter in terms of receptive field organization. This is illustrated in figure 15, which shows the component Gaussians of the DOG (figure 15a) and the DOG-s (figure 15c),

plotted with contrast sensitivity and spatial frequency on linear axes (dashed lines, centre mechanism; dotted lines, surround mechanism). The resultant combined functions, shown as solid lines in figure 15 a,c are replotted in figure 15 b,d, but in the more familiar log-log co-ordinates. The DOG function, with spatially co-incident peaks of the centre and surround mechanisms, obviously must have an individual Gaussian for the centre mechanism with a sensitivity that is greater than the peak of the resultant DOG. The sensitivity of the centre mechanism of the DOG is represented by the dashed line in figure 15b. In contrast, the DOG-s function, by virtue of the separation parameter, can attain the same peak sensitivity in the combined curve using Gaussians whose peaks are lower than their combination.

Text figure 15 near here

The centre Gaussian of the DOG-s function (figure 15d, dashed line) has a peak amplitude of 29, while the DOG-s function has a peak sensitivity of 43. This is because the effect of the surround Gaussian adds to that of the centre Gaussian at some spatial frequencies, owing to the difference in spatial phase introduced by the separation parameter (figure 15c,d). The two flanking regions forming the surround in the DOG-s model remain in even symmetric, cosine phase just like the single Gaussian mechanism forming the surround in the DOG model. Thus the Fourier transform of the DOG-s function has real parts only, which are illustrated in figure 15 c & d. This fundamental effect of the separation factor would help the visual system, using the DOG-s configuration, to create spatial contrast sensitivity functions with relatively narrow bandwidths, but without the attendant loss of sensitivity associated with narrow-band DOG functions (Marr & Hildreth 1980). These comments apply with even more force to the d-DOG-s model. Moreover, the addition of the spatial separation between centre and surround mechanisms, accounts for much of the improvement in the ability of the d-DOG-s and DOG-s models to fit the spatial contrast sensitivity functions, when compared with the DOG function. This is especially so, when the sensitivities of the individual Gaussians mechanisms have been constrained, as in the implementation of all three DOG-based models described in this paper. As will be seen later in the Discussion, the upper limit on the amplitude of the individual Gaussians is reasonable when consideration is given to the properties of lateral geniculate cells that must, directly or indirectly, provide input to the cortical cells.

As shown in figure 1, for the hypothetical spatial contrast sensitivity function, the inverse transform of the amplitude portion of the function can give spatial weighting profiles ranging from pure even symmetric to odd symmetric. Therefore it should be stressed that the best-fitting d-DOG-s functions do not uniquely specify the phase of the Fourier spectrum and therefore the relative strengths of the flanking regions. This point is exemplified in figure 16, which shows the versions of the d-DOG-s model that provide the best fit to the contrast sensitivity data of the cell shown in figures 6-10a, where the phase parameter (g) has been constrained to give a pure even symmetric (figure 16a), intermediate (figure 16b) or almost purely odd symmetric (figure 16c) profile. It can be seen, that although the relative amplitude and spatial organization of the surround component in the spatial weighting functions changes, the resultant amplitude spectra are almost identical.

Text figure 16 near here

Sub-units of cortical cell receptive field

A major advantage of the DOG-based models is that they can be interpreted in terms of the organization of the components of the receptive field. As mentioned in the section describing the DOG-based models, in order to maintain the parameters of these models within reasonable bounds, quite strong constraints were imposed during the curve-fitting procedures. For example, the maximum sensitivity of the individual Gaussians was constrained to be no greater than 1.5 times the greatest sensitivity recorded for each cell. Although the exact value of this limit is somewhat arbitary, the principle of setting a limit is very important. Otherwise, it would be possible for the DOG model to give a deceptively plausible description of a narrow-band spatial contrast sensitivity function, such as that in figure 13b. If the fitting procedure were allowed to hypothesize very high sensitivities ($>$250) for each Gaussian mechanism, the difference of the two would indeed be a high sensitivity, relatively narrow-band function, but the existence of single Gaussian mechanisms of very high sensitivity as real single entities in the nervous system is physiologically implausible and certainly not experimentally verified (Kaplan & Shapley 1982; Derrington & Lennie 1984).

In general, with the well-fitting DOG-s and d-DOG-s models, the parameters selected by the fitting procedure were well away from the bounds imposed by the constraints. In fact, the parameters selected by these models are highly compatible with the properties of lateral geniculate inputs (Kaplan & Shapley 1982; Derrington & Lennie 1984). For example, the centre mechanism space constants are in the range of 0.5 to 8.0 minutes of arc, for cells with receptive field centres within one degree of the fovea, and this range shifts systematically with eccentricity. Even for the small range of eccentricities studied in this work, the shift is evident and is similar to that seen for geniculate cells. Although these measures are derived from the application of a model, it should be stressed that they would be difficult to extract by other means. For example, the models separate out the differences in the sensitivities of the individual mechanisms from the differences in their spatial sizes. Further, use of the model gives some insight into how mechanisms could be combined to produce the overall receptive field profile. For example, figure 15 illustrates how inputs derived from parvocellular LGN cells, even though they generally have peak sensitivities lower than 25, could be used to build cortical cell receptive fields with a sensitivity higher than 25 at some spatial frequencies. Another mechanism for enhancing sensitivity in the cortex could be summation along the axis of preferred orientation. Finally, it is encouraging that some of the parameters of the receptive field are robustly defined even when results from different models are compared (see figures 6,7 and 8).

One of the remarkable features of our data is that no distinction can be drawn between simple and complex cells on the basis of the models describing their spatial contrast sensitivity functions. However, in terms of line weighting functions, there is a marked difference between the two cell classes in the cat cortex (Movshon et al. 1978a,b). There are several lines of evidence that suggest that complex cell receptive fields are made up of the non-linear combination of sub-units, which themselves show linear spatial summation (Movshon et al. 1978b; Spitzer & Hochstein 1985a,b). If these linearly summating sub-units have characteristics rather like simple cells in nearby areas of cortex, then it would be expected that no major differences between simple and complex cells would be found, in terms of their spatial contrast sensitivity functions. The similarity of simple cells and the

linearly summating sub-units of complex cells argues that they may have common sources of input from the LGN.

Anatomical considerations

A consequence of a relatively simple yet accurate model of the spatial weighting of striate neurons is that it allows some of the parameters to be tested against the anatomical distribution of inputs to cells. An intriguing feature suggested by the d-DOG-s and DOG-s models is that the peaks of some of the surrounds (or flanking regions) of receptive fields are separated from the centre mechanism by about 10 minutes of arc for cells with receptive fields within a degree of the foveal representation. A value of 10 minutes of arc with a magnification factor of 15mm/degree, which is perhaps a conservative estimate (Dow et al. 1981), indicates possible interactions, based on strict topographic order, over distances of 2-3mm across the cortex. Thus, there could well be a correlation between the orderly distribution of patch-like lattices seen in the anatomical arrangement of intra-cortical connections (Rockland et al. 1982) and the structure of the receptive fields. This would eliminate the need for any ill-defined concepts such as long range inhibitory influences or global 'pools' of non-specific inhibition in which cortical cells supposedly sit. Rather, the long-range connections can be seen as providing the anatomical basis for the straightforward, classically-defined and well documented features of receptive field organization.

Implications for visual processing

Cortical neurons display a wide variety of selectivities other than those defined in the models studied here. Thus the overall picture of cortical cell receptive fields provided by the models is incomplete, in that selectivity for direction and speed of motion, orientation, chromaticity or disparity is currently not included in the models. Despite the restricted nature of the models, some general conclusions about visual mechanisms can be made.

One consequence of using a poorly fitting model to process our results would be that the extraction of parameters of the function, such as bandwidth and peak frequency, would, in many cases, represent the data inaccurately. This might have serious consequences for the performance of a theoretical model of subsequent visual function that used the Gabor or D^2G for preliminary filtering. Furthermore, since a number of theoretical models of early visual processing underpin their use of the Gabor function by appealing to its property of minimizing conjoint uncertainty in space and spatial frequency, the failure of the Gabor function to match actual data from cortical cells suggests that this property is of limited significance for visual processing in the primate striate cortex. Whether the receptive fields of neurons in the extra-striate visual areas adhere to the Gabor shape or whether the characteristics of some cells in the striate cortex are close enough in shape to the Gabor function for its optimizing property to be adequately retained are matters for further experimental investigation. Rather similar points apply to D^2G and modifications of it (Marr & Hildreth 1980; Marr & Ullman 1981).

Our preferred models for cortical cell receptive field profiles are obviously not in accord with any previously proposed principles of computational vision (unlike, say, the use of ∇^2G functions to find zero crossings). The first stage in the application of such principles to a biological visual system must be an accurate model of the elements of the system. It is therefore worth considering what are the most marked differences between the shapes of filters, such as d-DOG-s, Gabor and D^2G. In the spatial frequency domain, two features are apparent. First,

cortical cells tend to have spatial contrast sensitivity functions that are roughly symmetric when plotted on a logarithmic frequency axis rather than a linear one. Gabor and D^2G functions are closer to symmetry on a linear frequency axis. A related feature is that the low-frequency cut of cortical cells is much steeper than either Gabor or D^2G would predict. Nonetheless, the bandwidths of cortical cells are not very narrow (DeValois et al. 1982). So appealing to a more narrowly tuned function, such as a higher order differential would not produce a significant improvement.

In the space domain, these features imply that the spatial extent of the receptive field, particularly its "inhibitory" flanking region, is greater than would be predicted from a Gabor or D^2G function. Prior to Marr and Hildreth's work on edge detection, the majority of edge detectors in computer vision systems worked on quite small regions of support (typically 3-6 pixels in linear extent). Marr and Hildreth (1980) introduced filters with considerably larger regions of support (approximately 30 pixels in linear extent). Adopting the d-DOG-s model suggests that the size should be bigger still for efficient edge detection and localization. Moreover, even when receptive fields have quite small centre mechanisms, they may have quite large "inhibitory" flanking regions.

The suitability of cortical receptive fields for edge detection and localization is emphasised by observations we have presented elsewhere. Localization thresholds for simple cells are in the hyperacuity range, both when measured directly or derived from calculations based on the DOG model of the receptive field (Parker & Hawken 1985), indicating that performance of individual neurons is well within the range found for human psychophysical observers. This is a case where the experimental determination of a spatial contrast sensitivity function followed by the application of a straightforward model of the receptive field results in testable predictions of the cell's behaviour.

Finally, it is obvious that the DOG-based models discussed here are similar, in many ways, to the original models of simple cells proposed by Hubel & Wiesel (1962). It has been suggested (DeValois et al. 1985) that the investigation of cortical cells with grating stimuli has revealed additional forms of receptive field organization that invalidate the Hubel & Wiesel model. It is ironic that the quantitative analysis presented here favours simple modifications of Hubel & Wiesel's model rather than schemes, such as the Gabor filters, that have been specifically inspired by the frequency domain approach to visual processing.

REFERENCES

Andrews, B.W. & Pollen, D.A. 1979 Relationship between spatial frequency selectivity and receptive field profile of simple cells. J. Physiol., Lond. 287, 163-176.

Bishop, P.O., Henry, G.H. & Smith, C.J. 1971 Binocular interaction fields of single units in the cat striate cortex. J. Physiol., Lond. 216, 39-68.

Blakemore, C & Campbell, F.W. 1969 On the existence of neurones in the human visual system selectively sensitive to the orientation and size of retinal images. J. Physiol., Lond. 203, 237-260.

Blakemore, C. & Vital-Durand, F. 1981 Distribution of X- and Y-cells in the monkey's lateral geniculate nucleus. J. Physiol., Lond. 320, 17-18P.

Braddick, O.J., Campbell, F.W. & Atkinson, J. 1978 Channels in vision: basic aspects. In Handbook of Sensory Physiology VIII, Perception, ed. R. Held, H.W. Leibowitz & H-L. Teuber. Heidelberg: Springer.

Campbell, F.W. & Robson, J.G. 1968 Application of Fourier analysis to the visibility of gratings. J. Physiol., Lond. 197, 551-566.

Cooper, G.F. & Robson, J.G. 1968 Successive transformations of visual information in the visual system. I.E.E. N.P.L. Conf. Proc. 42, 134-143. London: I.E.E.

Daugman, J.D. 1984 Spatial visual channels in the Fourier plane. Vision Res. 24, 891-910.

Daugman, J.D. 1985 Uncertainty relation for resolution in space, spatial frequency, and orientation optimized by two-dimensional visual cortical filters. J. opt. Soc. Am. A. 2, 1160-1169.

Dawis, S., Shapley, R.M., Kaplan, E. & Tranchina, D. 1984 The receptive field organization of X-cells in the cat: spatiotemporal coupling and asymmetry. Vision Res., 24, 549-564.

Dean, A.F. & Tolhurst, D.J. 1983 On the distinctness of simple and complex cells in the visual cortex of the cat. J. Physiol., Lond. 344, 305-325.

Derrington, A.M. & Lennie, P. 1982 The influence of temporal frequency and adaptation level on receptive field organization of retinal ganglion cells in the cat. J. Physiol., Lond. 333, 343-366.

Derrington, A.M. & Lennie, P. 1984 Spatial and temporal contrast sensitivities of neurones in the lateral geniculate nucleus of the macaque. J. Physiol., Lond. 357, 219-240.

DeValois, R.L., Albrecht, D.G. & Thorell, L.G. 1982 Spatial frequency selectivity of cells in macaque visual cortex. Vision Res., 22, 545-599.

DeValois, R.L., Thorell, L.G. & Albrecht, D.G. 1985 Periodicity of striate-cortex-cell receptive fields. J. opt. Soc. Am. A. 2, 1115-1123.

Dow, B.M., Snyder, A.Z., Vautin, R.G. & Bauer, R. 1981 Magnification factor and receptive field size in the foveal striate cortex of the monkey. Expl Brain Res., 44, 213-228.

Draper, N. & Smith, H. 1966 Applied Regression Analysis. New York: J. Wiley & Sons, Inc.

Eldridge, J.L. 1979 Reversible ophthalmoscope using a corner-cube. J. Physiol., Lond. 295, 1-2P.

Enroth-Cugell, C. & Robson, J.G. 1966 The contrast sensitivity of retinal ganglion cells of the cat. J. Physiol., Lond. 187, 517-552.

Enroth-Cugell, C., Robson, J.G., Schweitzer-Tong, D.E. & Watson, A.B. 1983 Spatio-temporal interactions in cat retinal ganglion cells showing linear spatial summation. J. Physiol., Lond. 341, 279-307.

Field, D.J. & Tolhurst, D.J. 1986 The structure and symmetry of simple-cell receptive-field profiles in the cat's visual cortex. Proc. R. Soc. B. 228, 379-400.

Gilbert, C.G. 1977 Laminar differences in receptive field properties of cells in cat primary visual cortex. J. Physiol., Lond. 268, 391-421.

Hawken, M.J. & Parker, A.J. 1984 Contrast sensitivity and orientation selectivity in lamina IV of the striate cortex of Old World monkeys. Expl Brain Res., 54, 367-372.

Heggelund, P. 1981 Receptive field organization of simple cells in cat striate cortex. Expl Brain Res., 42, 89-98.

Hochstein, S & Shapley, R.M. 1976 Quantitative analysis of retinal ganglion cell classifications. J. Physiol., Lond. 262, 237-264.

Hubel, D.H. & Wiesel, T.N. 1961 Integrative action in the cat's lateral geniculate body. J. Physiol., Lond. 155, 385-398.

Hubel, D.H. & Wiesel, T.N. 1962 Receptive fields, binocular interaction and functional architecture in cat's visual cortex. J. Physiol., Lond. 160, 106-154.

Hubel, D.H. & Wiesel, T.N. 1965 Receptive fields and functional architecture in two non-striate visual areas (18 & 19) of the cat. J. Neurophysiol., 28, 229-289.

Hubel, D.H. & Wiesel,T.N. 1968 Receptive fields and functional architecture of monkey striate cortex. J. Physiol., Lond. 195, 215-243.

Kaplan, E. & Shapley, R.M. 1982 X & Y cells in the lateral geniculate nucleus of macaque monkeys. J. Physiol., Lond. 330, 125-143.

Kulikowski, J.J. & Bishop, P.O. 1981 Linear analysis of the responses of simple cells in the cat visual cortex. Expl Brain Res., 44, 386-400.

Kulikowski, J.J., Marcelja, S. & Bishop, P.O. 1982 Theory of spatial position and spatial frequency relations in the receptive fields of simple cells in the visual cortex. Biol. Cybernet. 43, 187-198.

Levick, W.R. & Thibos, T.N. 1980 Orientation bias of cat retinal ganglion cells. Nature, 286, 389-390.

Linsenmeier, R.A., Frishman, L.J., Jakiela, H.G. & Enroth-Cugell, C. 1982 Receptive field properties of X and Y cells in the cat retina derived from contrast sensitivity measurements. Vision Res., 22, 1173-1183.

Marcelja, S. 1980 Mathematical description of the responses of simple co.tical cells. J. opt. Soc. Am. 70, 1297-1300.

Marr, D. 1982 Vision. San Francisco: W.H. Freeman & Co.

Marr, D. & Hildreth, E. 1980 Theory of edge detection. Proc. R. Soc. Lond. B. 207, 187-217.

Marr, D. & Ullman, S. 1981 Directional selectivity and its use in early visual processing. Proc. R. Soc. Lond. B. 211, 151-180.

Merrill, E.G. & Ainsworth, A. 1972 Glass-coated platinum-plated tungsten microelectrodes. Med. biol. Engng., 10, 662-672

Movshon, J.A., Thompson, I.D. & Tolhurst, D.J. 1978a Spatial summation in the receptive field of simple cells in the cat's striate cortex. J. Physiol., 283, 53-77.

Movshon, J.A., Thompson, I.D. & Tolhurst, D.J. 1978b Receptive field organization of complex cells in the cat's striate cortex. J. Physiol., 283, 79-99.

Parker, A.J. & Hawken, M.J. 1985 The capabilities of monkey cortical cells in spatial resolution tasks. J. opt. Soc. Am. A, 2, 1101-1114.

Parker, A.J. & Hawken, M.J. 1986 Threshold detection of luminance contrast by neurons in the primate striate cortex: a comparison with psychophysical performance (in preparation).

Robson, J.G. 1975 Receptive fields: spatial and intensive representations of the visual image. In: Handbook of Perception, Vol 5. Ed. D. Carterette & W. Friedman, pp 81-115. New York: Academic Press.

Robson, J.G. 1983 Frequency domain visual processing. In: Physical and Biological Processing of Images. Ed. O.J. Braddick & A.C. Sleigh, pp 73 - 87. Berlin: Springer-Verlag.

Rockland, K.S., Lund, J.S. & Humphrey, A.L. 1982 Anatomical banding of intrinsic connections in the striate cortex of tree shrews (Tupaia glis). J. comp. Neurol., 209, 41-58.

Rodieck, R.W. 1965 Quantitative analysis of cat retinal ganglion cell response to visual stimuli. Vision Res., 5, 583-601.

Rose, D. 1979 Mechanisms underlying the receptive field properties of neurons in cat visual cortex. Vision Res., 19, 533-544.

Sakitt, B & Barlow, H.B. 1982 A model for the economical encoding of the visual image in cerebral cortex. Biol. Cybernet., 43, 97-108.

Shapley, R.M., Kaplan, E. & Soodak, R.E.   1981 Spatial summmation and contrast sensitivity of X and Y cells in the lateral geniculate nucleus of the macaque. Nature, 292, 543-545.

Soodak, R.E. 1986 The spatial organization of visual receptive fields in the geniculostriate system of the cat. Ph.D. thesis, Rockefeller University.

Spitzer, H. & Hochstein,S. 1985a Simple- and complex-cell response dependences on stimulation parameters. J. Neurophysiol., 53, 1244-1265.

Spitzer, H. & Hochstein,S.   1985b A complex-cell receptive field model.   J. Neurophysiol., 53, 1266-1286.

Watson, A.B. 1983 Detection and recognition of simple spatial forms.   In: Physical and Biological Processing of Images. Ed. O.J. Braddick & A.C. Sleigh, pp 100 - 114. Berlin: Springer-Verlag.

Watt, R.J. & Morgan, M.J. 1985 A theory of the primitive code in human vision. Vision Res., 25, 1661-1674.

Wetherill, G.B. & Levitt, H. 1965 Sequential estimation of points on a psychometric function. Br. J. Math. & Statis. Psychol., 18, 1-10.

Wiesel, T.N. & Hubel, D.H. 1966 Spatial and chromatic interactions in the lateral geniculate body of the rhesus monkey. J. Neurophysiol., 29, 1115-1156.

Wilson, H.R. & Bergen, J.R. 1979 A four mechanism model for threshold spatial vision. Vision Res., 19, 19-32.

Yuille, A. & Poggio, T. 1985 Fingerprints theorems for zero-crossings. J. opt. Soc. Am., A2, 683-692.

APPENDIX

This appendix documents the equations used to describe the models and gives
some guidance on the interpretation of the parameters associated with the
models. The Fourier transform of these models is, in general, complex and the
amplitude portion of the Fourier transform was used to fit the measured
spatial contrast sensitivity function. However, because the line-weighting
function indicates the structure of the models much more clearly, the equation
specifying each model is the line-weighting function.

Models based on difference of Gaussian functions

These models consist of the algebraic sum of a number of Gaussian terms,
each of which is specified by a scaling factor (k_c, k_s etc.) and a space
constant (x_c, x_s, etc).

Units

x, x_c, x_s, S, etc. are measured in degrees of visual angle;

f is measured in cycles/degree;

k_c, k_s etc. are measured in the units: sensitivity deg.$^{-1}$ (see figures 6-10
right hand graphs).

The terms $k_c \sqrt{\pi} x_c$ etc., which appear in the Fourier transform, can be
usefully considered as a single constant with units corresponding to the
conventional measure of contrast sensitivity for grating stimuli. For
convenience, in the figure legends 6-10 the sensitivity constants are
expressed as a single value (e.g. A,B) in this way. The equivalences
between these two notations are indicated with the equations stating the
line-weighting function for each model.

Difference of difference of Gaussians with separation (d-DOG-S)

(1)
$$k_{c_1} \exp(-(x/x_{c_1})^2) - k_{s_1} \exp(-(x/x_{s_1})^2) -$$

$$g \cdot \left\{ k_{c_2} \exp(-((x+S)/x_{c_2})^2) - k_{s_2} \exp(-((x+S)/x_{s_2})^2) \right\} -$$

$$(1-g) \cdot \left\{ k_{c_2} \exp(-((x-S)/x_{c_2})^2) - k_{s_2} \exp(-((x-S)/x_{s_2})^2) \right\}$$

where the constraint

$$(k_{c_1} - k_{s_1}) - (k_{c_2} - k_{s_2}) = 0$$

is applied and the equivalences to Figure Legend 6 are

$$A_1 = k_{c_1} \sqrt{\pi}\, x_{c_1}; \quad A_2 = k_{s_1} \sqrt{\pi}\, x_{s_1}; \quad A_3 = k_{c_2} \sqrt{\pi}\, x_{c_2}; \quad A_4 = k_{s_2} \sqrt{\pi}\, x_{s_2};$$

Difference of Gaussians with separation (DOG-S)

(2)
$$k_c \exp(-(x/x_c)^2) - 0.5\, k_s \exp(-((x+S)/x_s)^2) -$$

$$0.5\, k_s \exp(-((x-S)/x_s)^2)$$

where the equivalences to Figure Legend 7 are

$$B_1 = k_c \sqrt{\pi}\, x_c; \quad B_2 = k_s \sqrt{\pi}\, x_s$$

Difference of Gaussians (DOG)

(3)
$$k_c \exp(-(x/x_c)^2) - k_s \exp(-(x/x_s)^2)$$

where the equivalences to Figure Legend 8 are

$$C_1 = k_c \sqrt{\pi}\, x_c; \quad C_2 = k_s \sqrt{\pi}\, x_s$$

Fourier transforms

The Fourier transform of the sum of a number of functions is simply the sum
of the Fourier transforms of those functions. The difference of Gaussian
models can therefore be treated by examining the contribution of individual
terms to the overall transform.

Terms of the form:

$$k_c \exp(-(x/x_c)^2)$$

have Fourier transforms of the form:

$$k_c \sqrt{\pi}\, x_c \, \exp\left(- \pi^2 f^2 x_c^2\right)$$

Terms of the form:

$$0.5\, k_s \, \exp\left(- ((x+S)/x_s)^2\right) \ + \ 0.5\, k_s \, \exp\left(- ((x-S)/x_s)^2\right)$$

have Fourier transforms of the form:

$$k_s \sqrt{\pi}\, x_s \, \exp\left(- \pi^2 f^2 x_s^2\right) \cdot \cos\left(2\pi f S\right)$$

An example of this behaviour is shown in figure 14.

Terms of the form:

$$0.5\, k_s \, \exp\left(- ((x+S)/x_s)^2\right) \ - \ 0.5\, k_s \, \exp\left(- ((x-S)/x_s)^2\right)$$

have Fourier transforms of the form:

$$k_s \sqrt{\pi}\, x_s \, \exp\left(- \pi^2 f^2 x_s^2\right) \cdot \sin\left(2\pi f S\right)$$

Gabor function

The Fourier transform of a Gabor function (a sinusoid multiplied by a Gaussian envelope) is a pair of Gaussian spectra centred at the frequency (f_c) of the sinusoid, one at $+f_c$, the other at $-f_c$. The relative signs of these spectra depend on the phase (p) of the sinusoid. If both are positive or both are negative, then the sinusoid is in cosine phase relative to the peak of the spatial Gaussian envelope. If one is positive and the other is negative, then the sinusoid is in sine phase. Note that this latter arrangement guarantees that a receptive field with this characteristic will have a zero sensitivity at zero spatial frequency.

(4) $k_c \, \exp\left(- (x/x_c)^2\right) \cdot \cos\left(2\pi f_c x + p\right)$

The constant D_l in figure legend 9 simply scales the height of the Gaussian spectra in the frequency domain, but it does not have a simple structural interpretation as do the constants for the DOG-based models.

Second differential of a Gaussian

The Fourier transform of this function can be understood most easily by

noting that a differentiation in the space domain is equivalent to multiplying the frequency spectrum by the complex quantity $2\pi jf$. The Fourier transform of the second differential of a Gaussian is therefore dominated by a quadratic term at low spatial frequencies and a Gaussian term at high spatial frequencies. The constant E_1 in figure legend 10 is simply a scaling factor.

(5) $\qquad (2k_c/x_c^2) \cdot (1 - 2x^2/x_c^2) \cdot \exp\left(- (x/x_c)^2\right)$

Table 1. The mean log. error per data point and F-ratio for the best-fitting version of each model to the spatial contrast sensitivity functions shown in figures 6 - 10.

	d-DOG-s	DOG-s	DOG	GABOR	D^2G
A.					
log. error	0.0013	0.0032	0.0097	0.0448	0.0933
F-ratio	4.5	4.69	12.5	60.6	94.9
	(4,134)	(8,134)	(9,134)	(9,134)	(11,134)
B.					
log. error	0.0018	0.0025	0.0053	0.0312	0.0591
F-ratio	15.7	9.3	17.4	84.7	152.7
	(3,124)	(7,124)	(8,124)	(8,124)	(10,124)

Table 2. The parameter values for the best-fitting version of d-DOG-s (a-f), DOG (g) and a single Gaussian (h) to the spatial contrast sensitivity functions shown in Figure 13.

Cell:	Sensitivity				Space Constant (min. arc)				Separation (min. arc) S	Symmetry g	Error	Lamina	Type (f_1/f_2)
	A_1	A_2	A_3	A_4	x_{c_1}	x_{s_1}	x_{c_2}	x_{s_2}					
a	48.7	14.8	39.1	4.4	4.07	5.99	8.40	33.6	12.5	0.5	0.0083	II/III	S(2.8)
b	97.8	97.7	97.8	97.7	7.59	13.1	7.29	14.3	8.88	0.5	0.0080	IVb	S(4.07)
c	20.0	20.0	20.0	20.0	1.79	12.1	5.45	15.4	9.88	0.5	0.0053	V	Cx(0.86)
d	20.5	15.2	9.5	7.1	2.73	5.56	3.02	11.7	7.38	0.5	0.0032	IVcα	S(1.63)
e	14.5	14.0	14.5	14.5	1.65	5.65	3.71	10.1	8.25	0.5	0.0135	II/III	Cx(0.92)
f	9.6	9.6	5.3	5.3	1.37	10.1	1.15	15.1	2.27	0.5	0.0054	IVcβ	Cx(0.73)
g	35.2	35.2			1.71	5.49					0.0063	VI	Cx(0.29)
h	14.1				4.62						0.0043	VI	S(4.03)

Figure 1

The upper graph (a) shows a bandpass function relating contrast sensitivity and spatial frequency, which is typical of the spatial contrast sensitivity functions found for most neurons in the striate cortex. The lower graphs show three possible inverse Fourier transforms of the amplitude spectrum in the upper graph, indicating the variations of receptive field organization consistent with this amplitude spectrum when no phase information is available. Left to right: purely even symmetry (b), intermediate (c) and purely odd symmetry (d).

Figure 2

Schematic representation of the individual Gaussian components and their combination for a receptive field model based on the difference of difference of Gaussians with separation (d-DOG-s, appendix: equation 1). Each sub-region of a receptive field is described by a difference of Gaussians function. Thus for a purely even symmetric field, with three sub-regions, there are six Gaussians altogether. For an odd symmetric field, with two sub-regions, there are only four Gaussians.
(a) Purely even symmetric field. The upper row shows an idealized 'hand-plotted' receptive field, with "on" centre (+) and "off" surround (-) sub-regions. The second row illustrates the individual Gaussians of each of the DOGs that make up the sub-regions of the d-DOG-s. The third row gives the spatial weighting function of the receptive field based on the linear combination of the three DOGs in the second row. (b) Odd symmetric receptive field. The upper row shows the hand-plotted receptive field with "on" and "off" sub-regions. The second row shows the individual Gaussians that make up the DOGs corresponding to the "on" and the "off" sub-regions in the upper row. The third row shows the form of the spatial weighting function that is the resultant of the two DOGs in the second row. It should be noted that the individual Gaussians of the "on" and "off" sub-regions do not necessarily have the same space constants and sensitivities. Consequently the resulting function, shown in the bottom row, need not be exactly odd symmetric.

Figure 3

(a) Schematic representation of the difference of Gaussians (DOG, appendix: equation 3), where the peaks of the two Gaussians are spatially co-incident. In this case the flanking sub-regions of the receptive field are formed by the spatial extremities of the surround Gaussian. The first row is the hand-plotted receptive field, the second row shows the component Gaussians of the centre ("on") region and the surround ("off") regions, while the third row gives the spatial weighting function based on the linear combination of the Gaussians in the second row. (b) Representation of the difference of Gaussians with separation (DOG-s, appendix: equation 2). The three rows are in the same sequence as described above for (a). This is equivalent to the purely even symmmetric version of the d-DOG-s model, where each sub-region is modelled by a single Gaussian rather than a DOG.

Figure 4

The distribution of 138 neurons on a test of the linearity of spatial summation. The receptive field of each neuron was stimulated with a temporally-modulated sine-wave grating at 12 different spatial phases. The amplitude of the second harmonic component of the impulse discharge (at twice the frequency of the temporal modulation) was averaged over all spatial phases to give the value f2. The value of f1 was determined at the spatial phase that gave the greatest fundamental response at the same frequency as the temporal modulation. Cells with f2/f1 ratios of less than

1 were considered to have a dominant linear component and have been classified as simple (77 cells), while those with f2/f1 ratios greater than 1, showing a dominant non-linear response, have been classified as complex (61 cells).

Figure 5
Relationship between mean contrast sensitivity and variance of measures of contrast sensitivity. The mean values of contrast sensitivity and the associated variance were obtained from 12 estimates using the staircase procedure described in the METHODS. For each cell, the mean and variance were calculated at every spatial frequency that yielded a significant response. Initially, the calculations were based on the assumption of a linear contrast scale (arithmetic mean and variance). The figure shows all these measurements pooled together. There is a positive relationship between arithmetic mean and variance with a slope of 1.85 as indicated by the solid line on the graph. A slope of 2 would indicate equal variance for logarithmically transformed values of contrast sensitivity.

Figure 6
The d-DOG-s model (appendix: equation 1) fitted to the contrast sensitivity functions (left) of two simple cells. The derived spatial weighting functions are shown on the right. Each determination of contrast sensitivity (unfilled circles) is the mean of 12 estimates from a staircase procedure; the error bars indicate +/- one standard deviation from the mean. The neuron whose sensitivity function is shown in (a) was recorded in layer VI of the striate cortex; the centre of the receptive field was located 1.2 degrees from the fovea. The neuron whose sensitivity function is shown in (b) was recorded in layer II in the same penetration. The values of the parameters of the best-fitting function are:
(a) $A_1 = 43$, $A_2 = 43$, $A_3 = 41$, $A_4 = 41$, $x_c = 2.22$ mins arc, $x_s = 15.36$ mins arc, $x_{c_2} = 4.97$ mins arc, $x_{s_2} = 17.41$ mins arc, $g = 0.25$, $S = 8.23$ mins arc. (b) $A_1 = 16$, $A_2 = 16$, $A_3 = 10$, $A_4 = 10$, $x_c = 2.23$ mins arc, $x_s = 16.10$ mins arc, $x_{c_2} = 4.41$ mins arc, $x_{s_2} = 27.46$ mins arc, $g = 0.5$, $S = 8.29$ mins arc.

Figure 7
The DOG-s model (appendix: equation 2) fitted to the contrast sensitivity functions of the same two cells as shown in figure 6. The details of the procedure and of the cells are given in figure 6. The values of the parameters of the best-fitting function are:
(a) $B_1 = 42.1$, $B_2 = 45.2$, $x_c = 2.21$ mins arc, $x_s = 4.58$ mins arc, $S = 7.38$ mins arc. (b) $B_1 = 15.0$, $B_2 = 16.6$, $x_c = 2.19$ mins arc, $x_s = 5.25$ mins arc, $S = 7.92$ mins arc.

Figure 8
The DOG model (appendix: equation 3) fitted to the contrast sensitivity functions of the same two cells as shown in figure 6. The details of the procedure and of the cells are given in figure 6. The values of the parameters of the best-fitting function are:
(a) $C_1 = 58.5$, $C_2 = 61.4$, $x_c = 2.38$ mins arc, $x_s = 10.14$ mins arc.
(b) $C_1 = 20.7$, $C_2 = 22.8$, $x_c = 2.45$ mins arc, $x_s = 11.54$ mins arc.

Figure 9
The Gabor model (appendix: equation 4) fitted to the contrast sensitivity functions of the same two cells as shown in figure 6. In almost all cases, the observed functions were more nearly symmetrical than the Gabor function plotted on logarithmic axes. The details of the procedure and of the cells are given in figure 6. The values of the parameters of the best-fitting function are:

(a) D_1 = 41.8, x_c = 1.94 mins arc, f_c = 2.92 c/deg., p = 90°. (b) D_1 = 23.8, x_c = 2.04 mins arc, f_c = 3.16 c/deg., p = 90°.

Figure 10

The D^2G model (appendix: equation 5) fitted to the contrast sensitivity functions of the same two cells as shown in figure 6. Like the Gabor function (figure 9), D^2G is not as symmetric as the data on logarithmic axes. The details of the procedure and of the cells are given in figure 6. The values of the parameters of the best-fitting function are:
(a) E_1 = 6.48, x_c = 3.49 mins arc. (b) E_1 = 2.87, x_c = 3.90 mins arc.

Figure 11

Relationship between the mean error per data point and the mean variance per data point for each of the models fitted to every cell in our sample. The filled symbols represent measurements from 77 simple cells, while the unfilled symbols are from 61 complex cells. The solid line in each graph, with a slope of 1, indicates where the error is equal to the variance. A point below the diagonal line indicates that the error in fitting the model to the data is less than the variance associated with the sensitivity measurements for that cell. Conversely points above the line indicate that the error was greater than the variance; such points indicate cells that are relatively poorly fit by the model. We have arranged the models from best to worst, based on the number of data points above the line of equality; the order is d-DOG-s (a), DOG-s (b), DOG (c), Gabor (d) and D^2G (e).

Figure 12

The mean error per data point for the best-fitting version of the d-DOG-s model (ordinate) is plotted against the mean error per data point for the other four models. Deviations below the solid line of equal error indicate a failure of the model represented on the abscissa to account for the spatial contrast sensitivity function as well as the d-DOG-s model. The filled and unfilled symbols indicate simple and complex cells respectively, as in figure 11.

Figure 13

Panels (a-f) show the d-DOG-s model (appendix: equation 1) fitted to the contrast sensitivity functions of six neurons, in order to illustrate the variety of shapes of these functions and the ability of the model to describe them. The lowest two panels show examples of cells that were well fitted by the DOG model (g) and by a single Gaussian (h). Details of the parameters are given in table 2. The open circles indicate the mean value of contrast sensitivity and the error bars indicate +/- one standard deviation from the mean. Cells in a,b,c,e had receptive fields between 1.0 and 1.5 degrees from the fovea; receptive fields of cells in d,f,g were within 0.5 degrees of the fovea; receptive field of cell in h was 3.0 degrees from the fovea.

Figure 14

The upper two graphs show the contrast sensitivity function from one of the few neurons for which the Gabor (a) shows a significantly better fit than the simple DOG (b). The mean error associated with the Gabor fit is 0.0028 and with the DOG 0.0131. However, the DOG-s model (c) can fit the data with a similar error to the Gabor, 0.0023. The cell was classified as simple, with a receptive field 0.4 degrees from the fovea, and was recorded in layer IVc . (d) Comparison of the mean error obtained from the best-fitting versions of the DOG and the Gabor functions for all cells. The details are the same as for figure 12.

Figure 15

(a) The centre (dashed line) and surround (dotted line) Gaussians of a DOG function plotted on linear spatial frequency and contrast sensitivity axes. Because the peaks of the centre and surround Gaussians are spatially co-incident, they subtract at all spatial frequencies. Therefore, to obtain a DOG of a given amplitude, the centre mechanism's sensitivity must be greater than the maximum sensitivity of the DOG. The combination of the centre and surround is shown by the solid line in (a). In (b) the solid line shows the same DOG as in (a), but on the more familiar log-log axes, while the centre mechanism is shown by the dashed line. In (c) the centre (dashed line) and surround (dotted line) Gaussians of a DOG-s (solid line) function are shown on linear axes. The same DOG-s function as seen in (c) is shown in (d) on log-log axes. Note that the surround Gaussian is of the same sign as the centre Gaussian at some spatial frequencies (see Appendix). Thus the two Gaussians combine their sensitivities at these spatial frequencies with the result that the peak sensitivity attained by the DOG-s function, shown by the solid line in (c and d), is greater than the centre component alone (dashed line in c and d).

Figure 16

The graphs show the versions of the d-DOG-s model that fit best to the contrast sensitivity data of the cell in figure 6a, where the model varies from: (a) pure even symmetry, the symmetry parameter $g = 0.5$; (b) through intermediate symmetry, $g = 0.26$; (c) to almost pure odd symmetry, $g = 0.0$. (See figure legend 3.) All the other parameters were free to vary. The figure shows that, within the constraints of the d-DOG-s model, the relative amplitudes and spatial organization of the flanking sub-regions may change without any marked change in the amplitude spectrum. It is worth noting that the separation parameter stays almost constant, at around 8 mins. of arc, in all three fits despite the change of symmetry of the flanking regions.

Figure 1
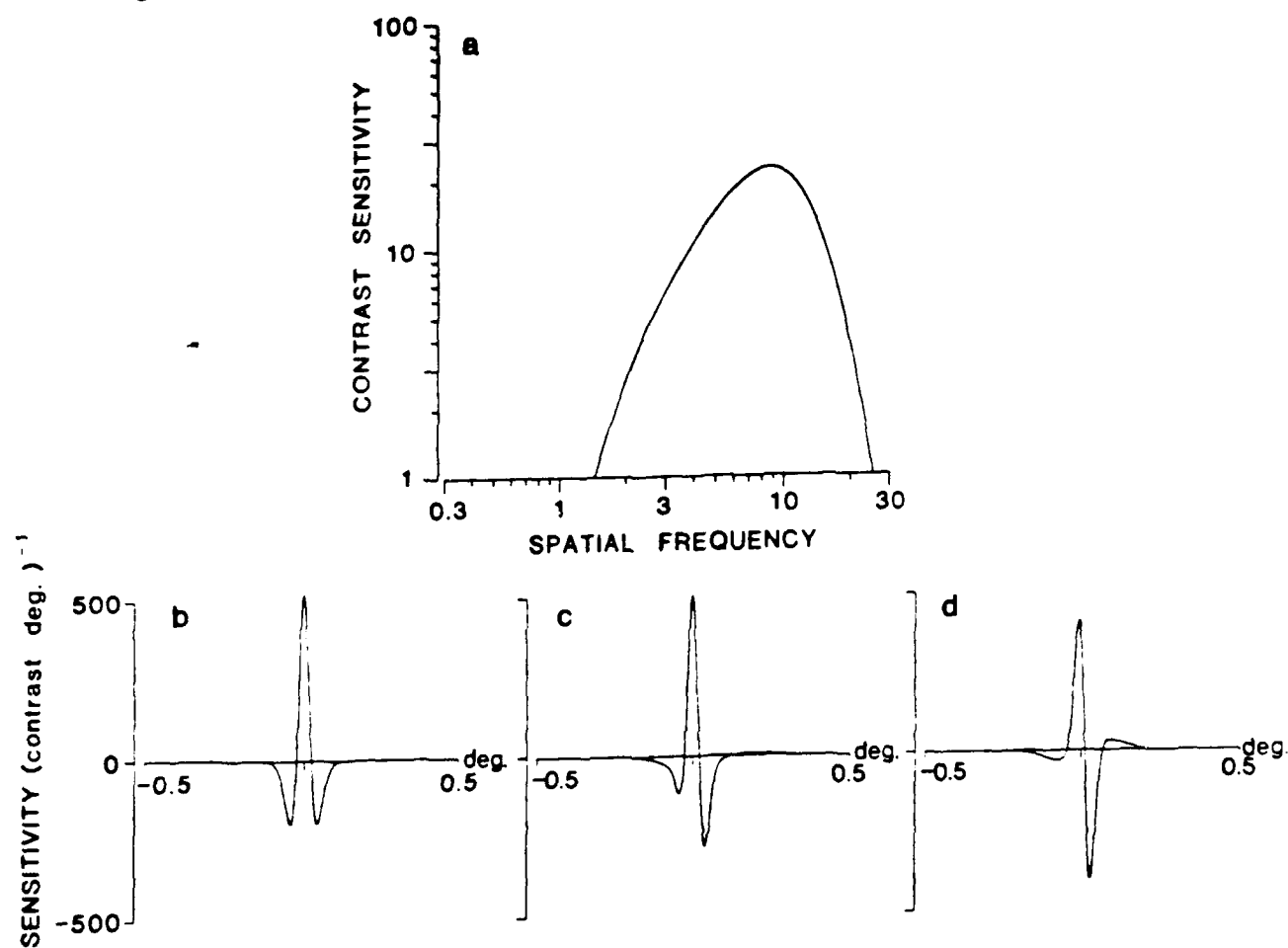
Figure 2
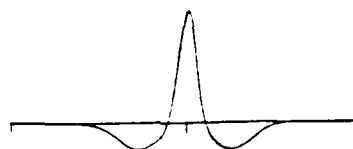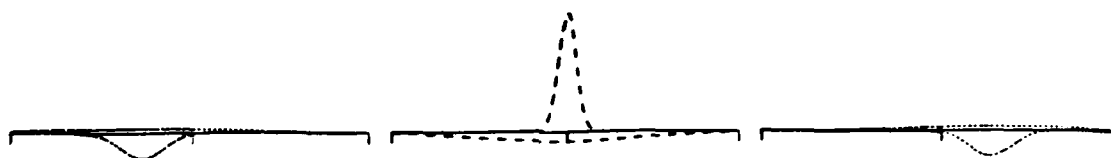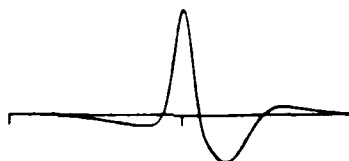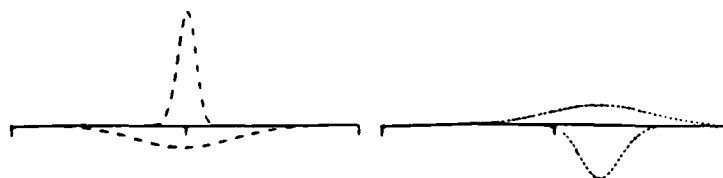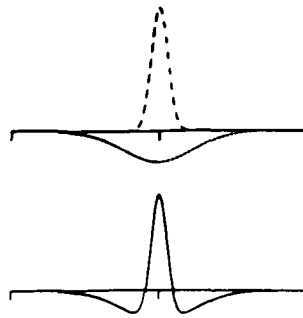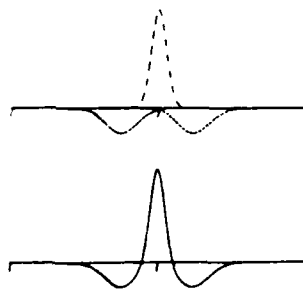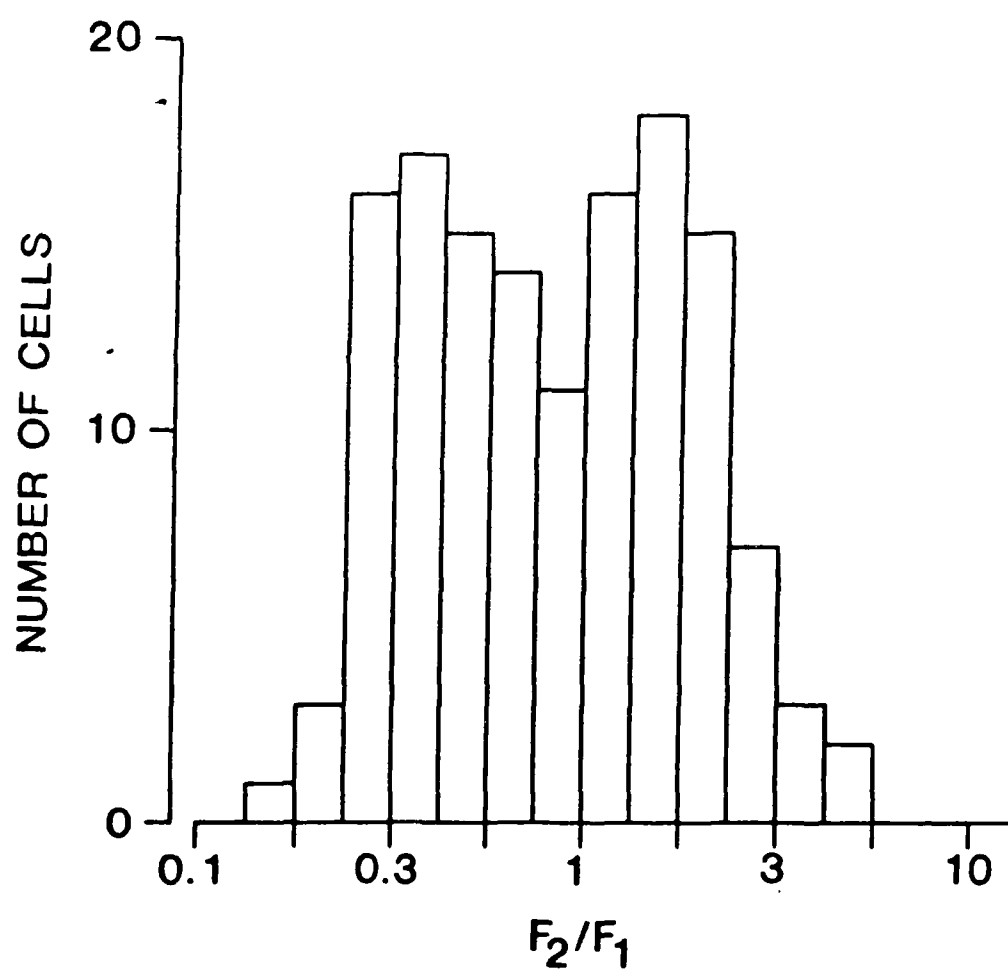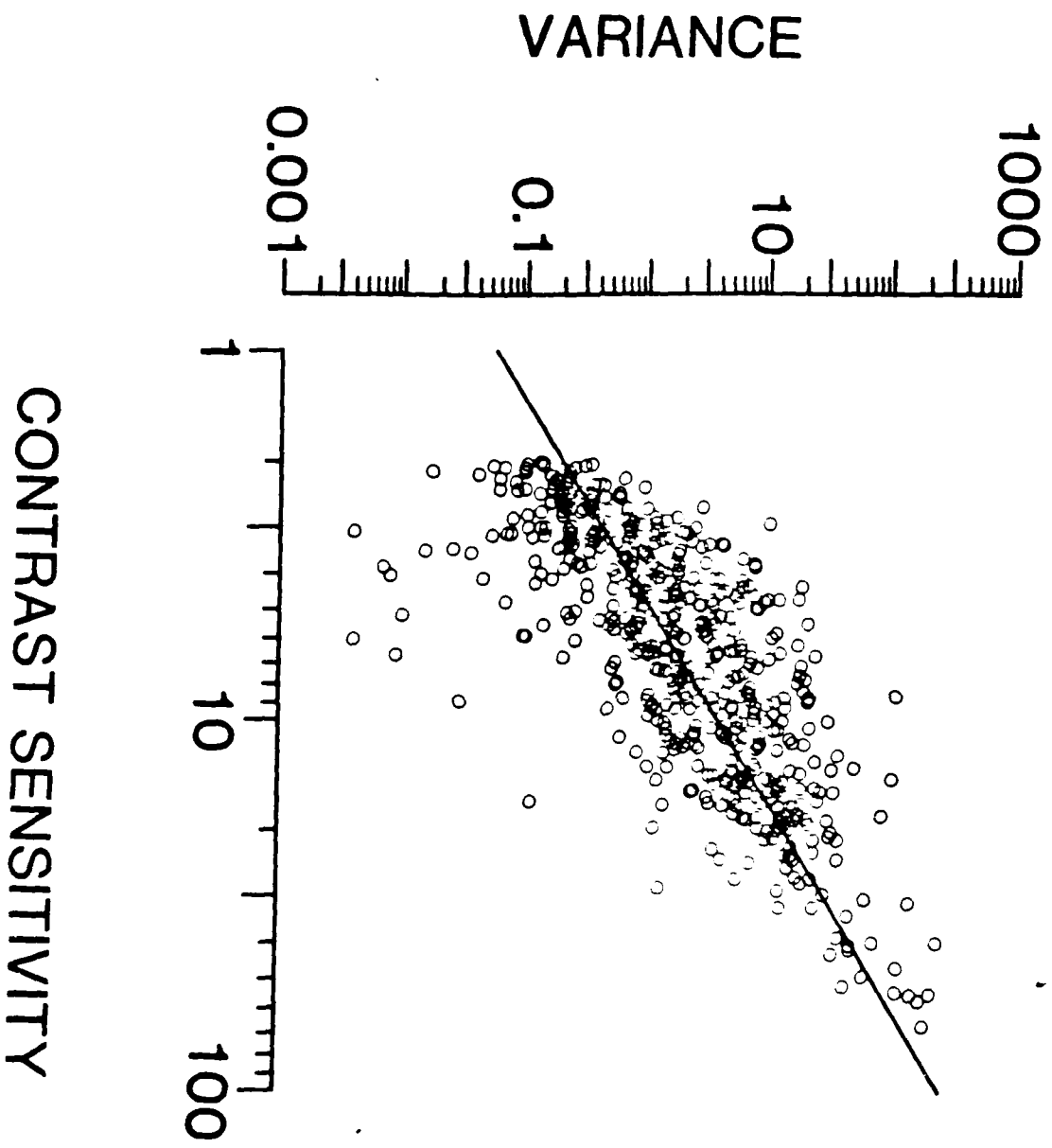
Figure 4

Figure 5

Figure 6
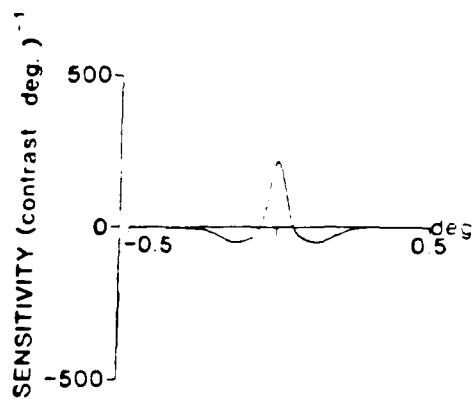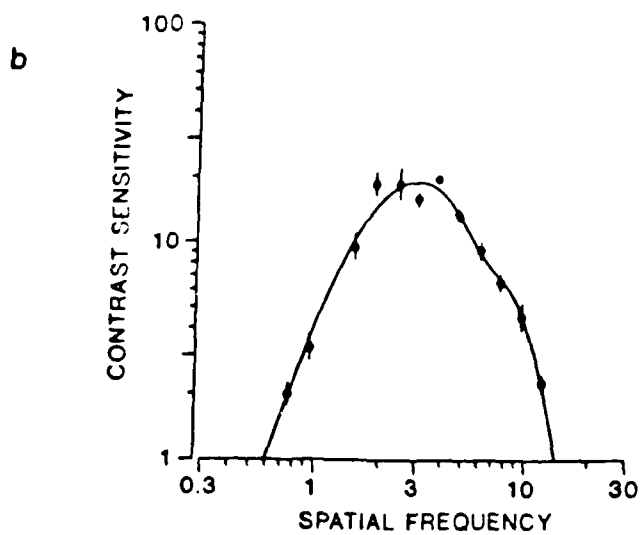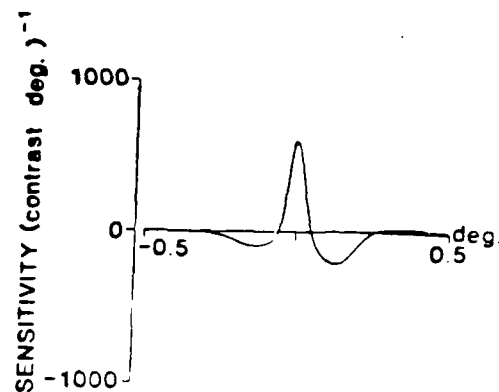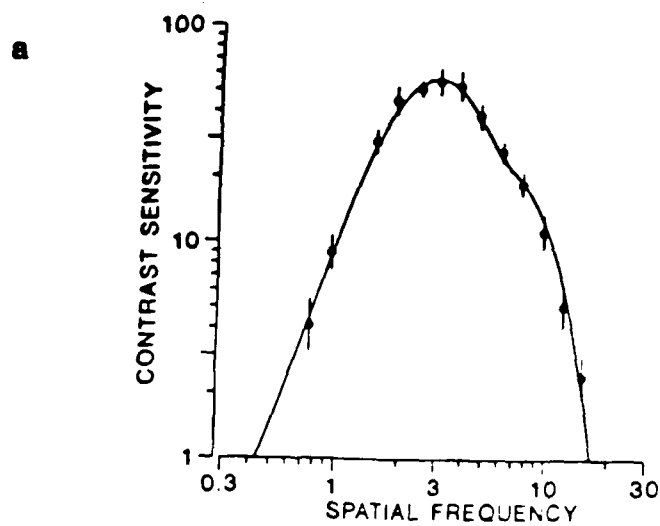
Figure 7

a

b

Figure 8

Figure 9

a

b
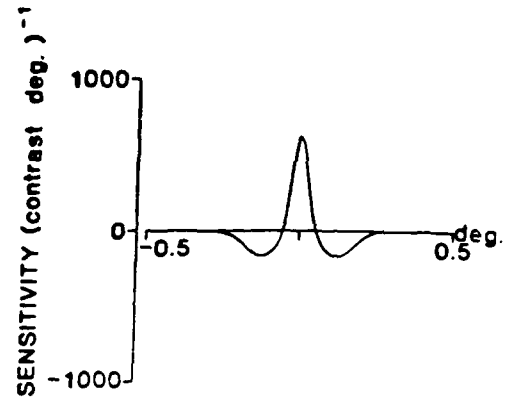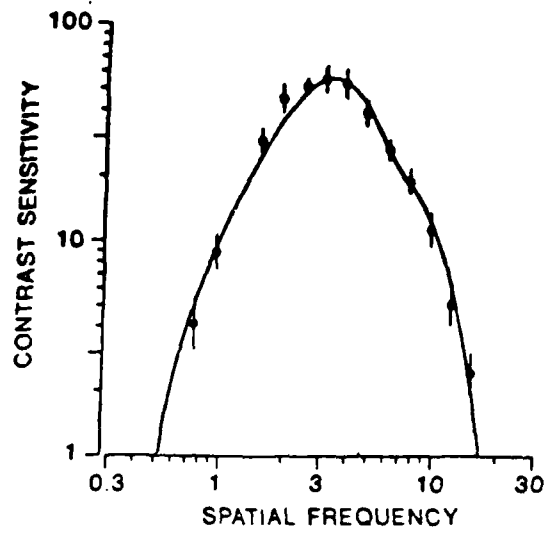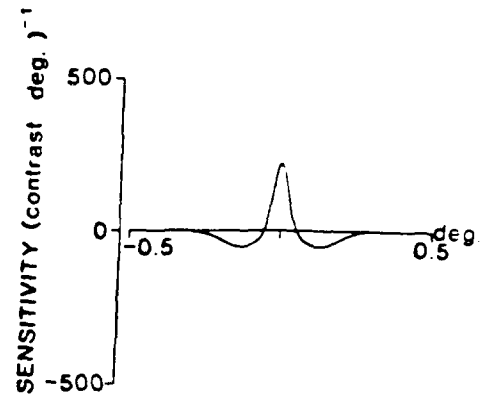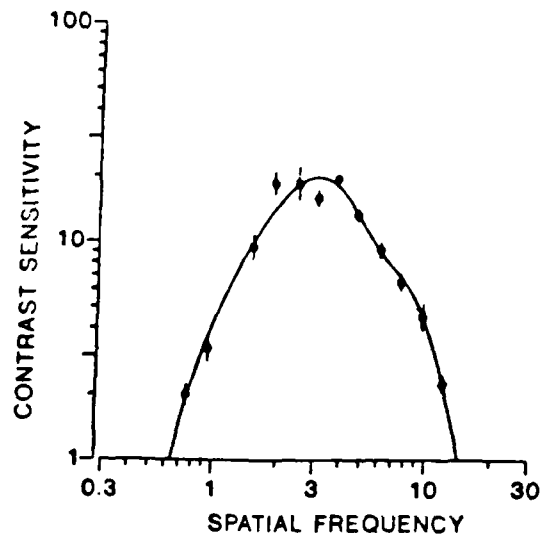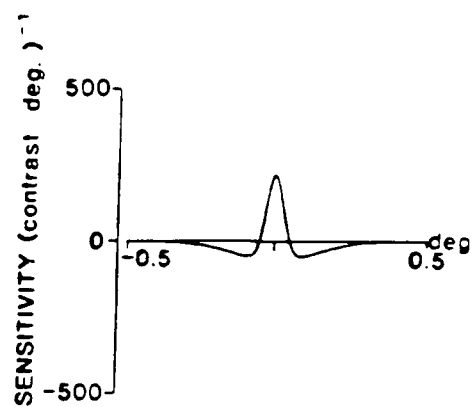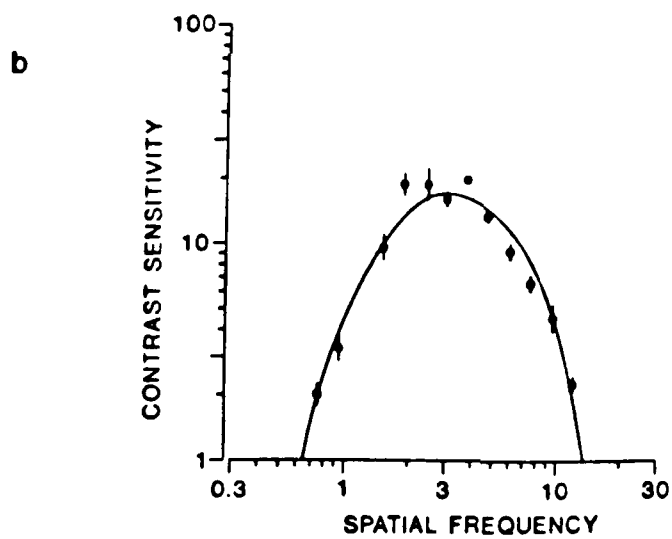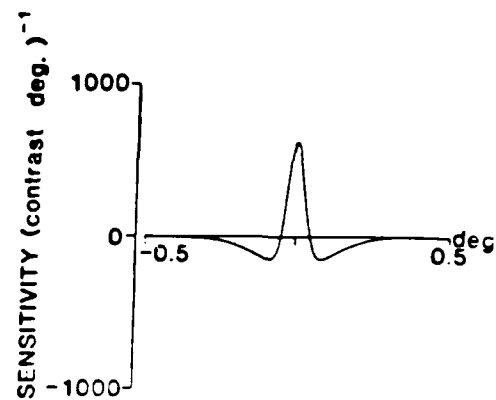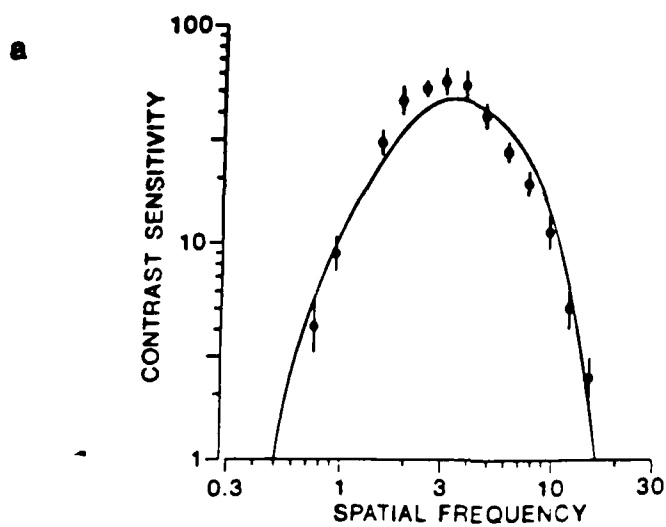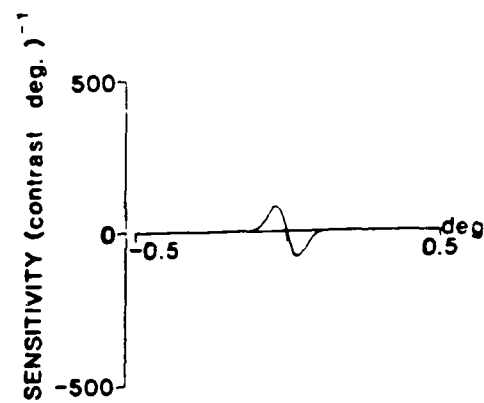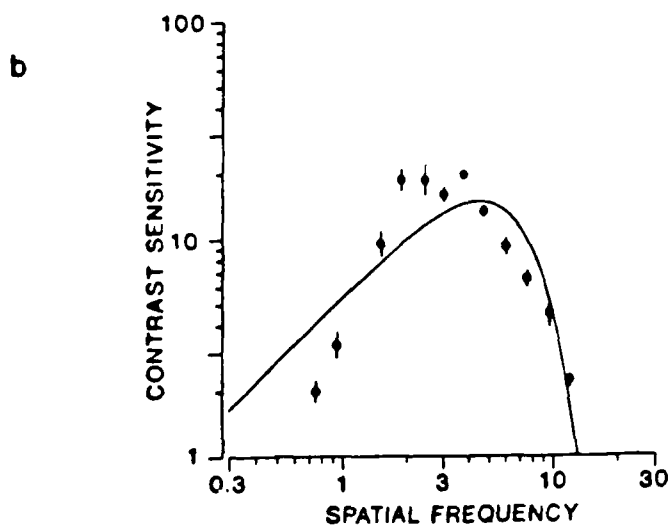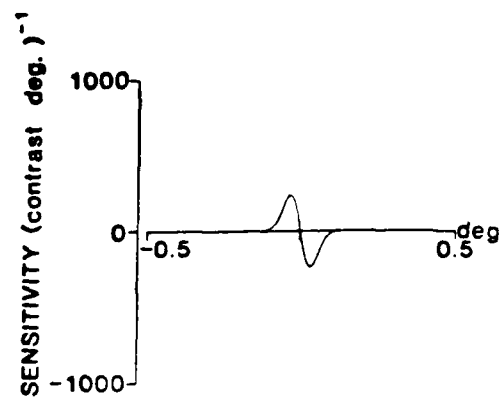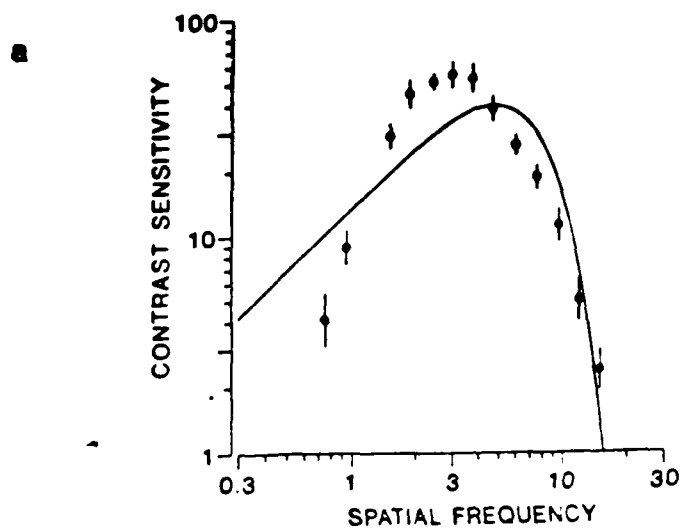
Figure 10

Figure 12

Figure 13

Fig 14

Fig 15

Figure 16

DO NOT FOLD THIS F(
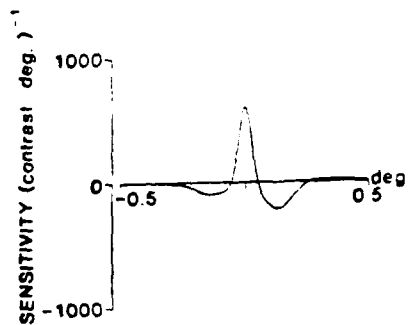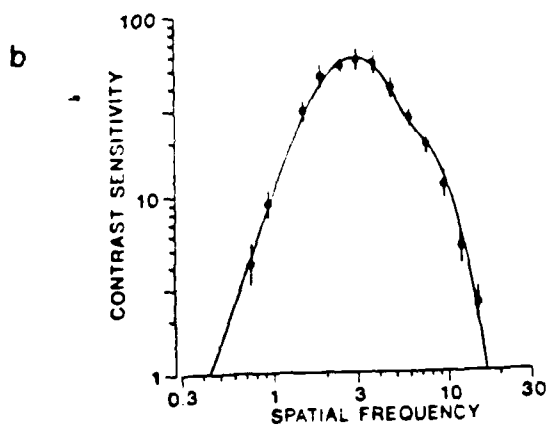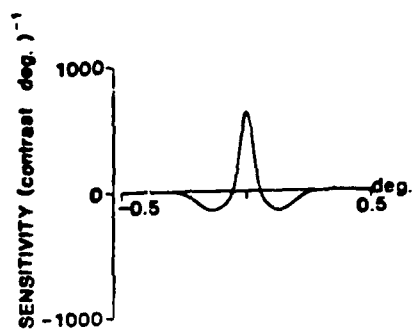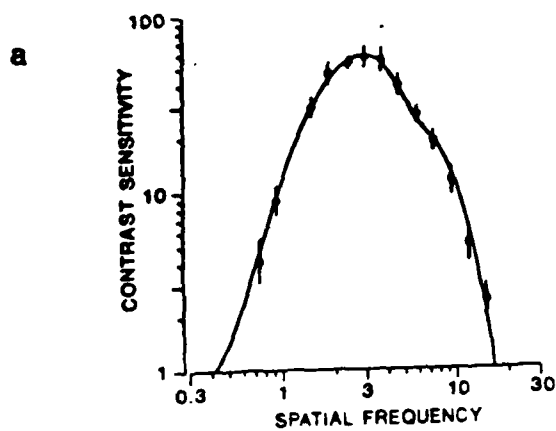
987 ARVO ABSTRACT FORM

FOR OFFICE USE ONLY

Presentation Preference

'lease check one
_____ Paper only or Withdraw
_____ Poster only or Withdraw
_____ Paper or Poster
(no preference)
_X_ Paper #1, Poster #2
_____ Poster #1, Paper #2

Scientific Section Preference

see section description on page 3
ndicate below a 1st and 2nd choice for
our presentation
_____ Anatomy & Pathology
_____ Biochemistry
_____ Clinical Research
_____ Cornea
_1_ Electrophysiology
_____ Eye Movements, Strabismus
& Amblyopia
_____ Glaucoma
_____ Immunology & Microbiology
_____ Lens
_____ Physiology & Pharmacology
_____ Retina
_____ Retinal Cell Biology
_2_ Visual Psychophysics

ecial Requirements (eg overhead/
ovie projector, shared expenses of
eo equipment, etc)

CONTRAST SENSITIVITY AND LAMINAR DISTRIBUTION OF DIRECTION SENSITIVE NEURONS IN MONKEY STRIATE CORTEX. M.J. Hawken, A.J. Parker & J.S. Lund* Dept. of Physiology, Univ. of Oxford, UK. & *Dept. of Psychiatry, Univ. of Pittsburg, USA.

In many circumstances, when a moving stimulus is detected psychophysically then the direction of motion can also be identified. This suggests that the same mechanism is responsible for the detection of a moving stimulus and for the identification of its direction of motion. The striate cortex is the first area in the visual pathway where there are substantial numbers of direction selective neurons which could be the neural basis of the proposed psychophysical mechanism. For neurons in all layers of the striate cortex, we have measured both the contrast sensitivity and the magnitude of direction preference for moving achromatic gratings of optimal orientation and temporal frequency. Those neurons with a substantial bias for direction are confined to the upper sub-layers of layer 4 (4a, 4b & 4cα) and layer 6; the majority of these are simple cells. Over the low and middle ranges of spatial frequency, the peak contrast sensitivities of the directionally selective cells are among the highest found in the striate cortex. These results suggest that there is a population of cells that have low contrast thresholds and that are selective to the direction of stimulus motion, just as proposed on the basis of psychophysical studies. Furthermore, many of these directionally selective cells are located in layers of the striate cortex that provide direct input to extrastriate area MT which is involved in the processing of visual motion.

MPORTANT

Type abstract carefully on this form only,
using a clear black carbon ribbon

Also fill out
• Presentation preference
• Scientific section preference
• First author
• Sponsoring author
• Reverse side - copyright transfer

Return to ARVO by Dec 10, 1986
• 1 original blue abstract form
• 6 copies
• return stamped postcards
• travel grant application
(if appropriate)

MPLETE FORM ON REVERSE SIDE

First (presenting) Author

Provide full name, address and phone numbers of 1st author on abstract. You may present only one abstract

HAWKEN   MICHAEL   JOHN

Dept. of Physiology, Parks Road   First   Middle

Oxford, Address OX1 3PT   U.K.

(0865) 57451   State   (0865) 67138   Country

Office Phone Number   Home Phone Number

☐ Member
☒ Applying Member (Application enclosed)
☐ Non Member

Membership No (look on mailing label)

Sponsor (must be member if 1st author is not)

Provide full name of sponsoring member, phone number and signature. You may sponsor only one abstract, a only if you are not the presenting author of another abstract

Last   First   Middle

Office Phone Number   Home Phone Number

Signature   Membership No (look on mailing label)

1987 ARVO ABSTRACT FORM

DO NOT FOLD THIS FORM

FOR OFFICE USE ONLY

Presentation Preference

Please check one
_____ Paper only or Withdraw
__✓__ Poster only or Withdraw
_____ Paper or Poster
        (no preference)
_____ Paper #1, Poster #2
_____ Poster #1, Paper #2

Scientific Section Preference

See section description on page 3
Indicate below a 1st and 2nd choice for your presentation
_____ Anatomy & Pathology
_____ Biochemistry
_____ Clinical Research
_____ Cornea
_____ Electrophysiology
2 ✓ Eye Movements, Strabismus & Amblyopia
_____ Glaucoma
_____ Immunology & Microbiology
_____ Lens
_____ Physiology & Pharmacology
_____ Retina
_____ Retina Cell Biology
1 ✓ Visual Psychophysics

Special Requirements (eg overhead/ movie projector, shared expenses of video equipment, etc)

IMPORTANT

1. Type abstract carefully, on this form only, using a clean black carbon ribbon

2. Also fill out
   • Presentation preference
   • Scientific section preference
   • First author
   • Sponsoring author
   • Reverse side - copyright transfer

3. Return to ARVO by Dec 10, 1986
   • 1 original blue abstract form
   • 6 copies
   • return stamped postcards
   • travel grant application
     (if appropriate)

COMPLETE FORM ON REVERSE SIDE

SPATIAL PROPERTIES OF A DISPARITY POOLING PROCESS
Yuede Yang & Andrew Parker, Physiology Dept., Univ. of Oxford, UK

A number of psychophysical and computational studies point to the existence of processes concerned with combining local information from individual disparity-detecting elements into a globally consistent interpretation. The spatial limits of disparity averaging were investigated using Julesz random-dot stereograms (RDS) with two surfaces embedded within each stereopair. At some disparities, such stimuli are perceived as two separate surfaces, one of which is seen through the transparent veil of the other, but under some conditions the depth information provided by the two surfaces is pooled and the resulting surface is seen at the average of the local disparities. 2AFC thresholds were obtained for discriminating the relative depths of two rectangular regions of fronto-parallel surface within the RDS. In the test region, the even-numbered rows of dots signalled one disparity and the odd-numbered rows signalled a different disparity; in the comparison region, there was only one disparity value. With small disparity differences, the perceived depth of the test target was judged to be the average of the two components. Disparity averaging breaks down with large differences in the disparity of the two components, but the tolerable range of disparity differences increases as the average disparity of the components relative to the background increases. Averaging was also obtained with slanted surfaces, but the effect appears over a wider range of disparities. The results suggest the existence in human vision of a process of interpolation over surfaces in depth.

First (presenting) Author

Provide full name, address and phone numbers of 1st author on abstract. You may present only one abstract

Yang	Yuede	
Last	First	Middle
University Lab. of Physiology, Parks Road,		
Street Address:		
Oxford, OX1 3PT	England	UK
City,	State	Country
+44 865 272 506		
Office Phone Number		Home Phone Number

☐ Member
✗ Applying Member (Application enclosed)
☐ Non Member

Membership No (look on mailing label)

Sponsor (must be member if 1st author is not)

Provide full name of sponsoring member, phone number and signature. You may sponsor only one abstract, and only if you are not the presenting author of another abstract.

Last	First	Middle
Office Phone Number		Home Phone Number
Signature		Membership No (look on mailing label)

1987 ARVO ABSTRACT FORM

FOR OFFICE USE ONLY

Presentation Preference

Please check one
_____ Paper only or Withdraw
_____ Poster only or Withdraw
_____ Paper or Poster
       (no preference)
__X__ Paper #1, Poster #2
_____ Poster #1, Paper #2

Scientific Section Preference

See section description on page 3
Indicate below a 1st and 2nd choice for your presentation

_____ Anatomy & Pathology
_____ Biochemistry
_____ Clinical Research
_____ Cornea
__2__ Electrophysiology
_____ Eye Movements, Strabismus
       & Amblyopia
_____ Glaucoma
_____ Immunology & Microbiology
_____ Lens
_____ Physiology & Pharmacology
_____ Retina
_____ Retinal Cell Biology
__1__ Visual Psychophysics

Special Requirements (eg overhead/movie projector, shared expenses of video equipment, etc.)

IMPORTANT

1 Type abstract carefully, on this form only, using a clean **black** carbon ribbon

2 Also fill out
   • Presentation preference
   • Scientific section preference
   • First author
   • Sponsoring author
   • Reverse side - copyright transfer

3 Return to ARVO by Dec 10, 1986
   • 1 original blue abstract form
   • 6 copies
   • return stamped postcards
   • travel grant application
     (if appropriate)

COMPLETE FORM ON REVERSE SIDE

SURFACE CURVATURE AS A DESCRIPTOR OF THREE DIMENSIONAL SHAPE
Elizabeth Johnston and Andrew Parker
University Laboratory of Physiology, Oxford, England.

Current models in computational vision make use of differential geometry to describe the properties of three dimensional surfaces. These psychophysical experiments with Julesz random dot stereograms were designed to measure the stereoscopic sensitivity of human observers to changes in the curvature of three dimensional surfaces A 2AFC technique was used to determine curvature thresholds for surfaces of zero Gaussian curvature (portions of cylinders). With a 50 min.arc radius (curvature : 0.02 rad/min.arc), the 75% discrimination threshold was a 13 min.arc change in radius. With larger radii discrimination was poorer. To use Gaussian curvature to analyse the shape of a surface observers must possess a basic sensitivity to the principal axes of curvature. This was tested using a 2AFC paradigm, in which subjects decided which of the two principal axes of curvature on a surface with positive Gaussian curvature had the higher curvature. This corresponds to discriminating an ellipsoid from a sphere. Thresholds obtained for this task were highly similar to those measured in experiment one. Thus, the values of the principal axes of curvature are available to subjects within the limits of curvature acuity. For surfaces with negative Gaussian curvature (hyperbolic paraboloids) thresholds were at least 8 min.arc higher at each radius tested. Further differences in sensitivity to surfaces with different sign of Gaussian curvature were noted in the third experiment, in which a masking paradigm was used to obtain detection thresholds for a number of surfaces. Surfaces of positive Gaussian curvature tolerated much greater noise perturbation than surfaces with negative Gaussian curvature.

First (presenting) Author

Provide full name, address and phone numbers of 1st author on abstract. You may present only one abstract

Last	First	Middle
Johnston	Elizabeth	Buchanan

Street Address
University Laboratory of Physiology, Parks Road,

City	State	Country
Oxford	OX1 3PT	England

Office Phone Number	Home Phone Number
0865 57451	0865 245285

☐ Member
☒ Applying Member (Application enclosed)   Membership No (look on mailing label)
☐ Non Member

Sponsor (must be member if 1st author is not)

Provide full name of sponsoring member, phone number and signature. You may sponsor only one abstract and only if you are not the presenting author of another abstract

Last	First	Middle

Office Phone Number   Home Phone Number

Signature   Membership No (look on mailing label)

DO NOT FOLD THIS FORM

1987 ARVO ABSTRACT FORM

FOR OFFICE USE ONLY

Presentation Preference

Please check one
_____ Paper only or Withdraw
_____ Poster only or Withdraw
_____ Paper or Poster
      (no preference)
_____ Paper #1, Poster #2
__X__ Poster #1, Paper #2

Scientific Section Preference

See section description on page 3
Indicate below a 1st and 2nd choice for
your presentation
__X__ Anatomy & Pathology
_____ Biochemistry
_____ Clinical Research
_____ Cornea
_____ Electrophysiology
_____ Eye Movements, Strabismus
       & Amblyopia
_____ Glaucoma
_____ Immunology & Microbiology
_____ Lens
_____ Physiology & Pharmacology
_____ Retina
_____ Retinal Cell Biology
_____ Visual Psychophysics

Special Requirements (eg overhead/
movie projector, shared expenses of
video equipment, etc.)

MPORTANT

1 Type abstract carefully, on this form only,
  using a clean black carbon ribbon

2 Also fill out
  • Presentation preference
  • Scientific section preference
  • First author
  • Sponsoring author
  • Reverse side — copyright transfer

3 Return to ARVO by Dec 10 1986
  • 1 original blue abstract form
  • 6 copies
  • return stamped postcards .
  • travel grant application
    (if appropriate)

COMPLETE FORM ON REVERSE SIDE

LOCAL CIRCUIT NEURON ORGANIZATION IN INFRAGRANULAR LAYERS OF MONKEY STRIATE VISUAL CORTEX. J.S. Lund, M.J. Hawken* and A.J. Parker*. Department of Psychiatry, University of Pittsburgh and *Department of Physiology, Oxford.

Layers 5 and 6 of striate cortex contain all the subcortically projecting efferent neurons of this region plus neurons providing important efferent projections to extrastriate visual cortex. The local circuit (LC) neurons of these layers (characterized by their smooth or sparsely spined dendrites and predominantly GABAergic nature) must play a vital role in determining the outflow of visual information and intrinsic patterning of activity in these deep layers. We have studied the organization of the LC neurons using Golgi impregnations in infant monkey cortex where the interlaminar axon projections of the LC neurons can be traced; myelination in older animals prevents silver impregnation of these relays. We find a rich variety of LC neurons; each variety has highly specific patterns of axon distribution – both within and between divisions of the infragranular layers 5 and 6 and in projections to both supragranular layers and thalamic recipient divisions of lamina 4. These relays illustrate important pathways by which layers 5 and 6 interact and influence activity more superficially in the cortex. The patterns of these relays can be compared to the internal axon distribution of pyramidal neurons of layers 5 and 6 and it is clear that there is considerable relationship in the pattern of relays by these excitatory and inhibitory neuron groups.

First (presenting) Author

Provide full name, address and phone numbers of 1st author of abstract. You may present only one abstract

Lund, Jennifer S.
Last / First / M ddle

University of Pittsburgh, 336C Scaife Hall
Street Address

Pittsburgh, PA U.S.A.
City / State / Country

412-648-9044 412-682-7544
Office Phone Number / Home Phone Number

☒ Member 22033
☐ Applying Member (Application enclosed) Membership No (look on mailing label)
☐ Non Member

Sponsor (must be member if 1st author is not)

Provide full name of sponsoring member, phone number and signature. You may sponsor only one abstract, and only if you are not the presenting author of another abstract

La Fi M ddle

Office Phone Number / Home Phone Number

2-D STRUCTURE OF CORTICAL MECHANISMS FOR CONTRAST DETECTION

Andrew Parker & Mike Hawken, Physiology Dept., Oxford, UK

The shapes of receptive fields of neurons in the primate
striate cortex suggest that they could be the mechanisms
underlying the spatial channels identified in psychophysical
contrast detection experiments. Analysis of the spatial
contrast sensitivity functions of striate neurons shows that the
most comprehensive description of their behaviour is given by a
2-dimensional model, consisting of the algebraic sum of up to 3
difference-of-Gaussian (DOG) functions in the axis orthogonal
to the preferred orientation of the cell and a single Gaussian
function in the direction parallel to this axis. For simple
cells, each major excitatory or inhibitory zone of the
receptive field is served by one DOG function. The space
constants of the smallest 'centre' mechanisms are in the range
1 to 8 min arc for eccentricities of 1.5 degrees or less. Even
when the 3-DOG model is restricted to only 4 or 5 free
parameters, it gives significantly more accurate descriptions
of contrast sensitivity functions than either the Gabor
function or the 2nd differential of a Gaussian. The space
constant of the single Gaussian describing the axis parallel to
the preferred orientation can be derived from the orientation
selectivity of the cell. The values fall in the range 3 to 35
min arc, but are more conveniently specified as a ratio
relative to the overall width of the receptive field, measured
from the extremities of the flanks of the receptive field. The
modal value of this ratio is about 1 and nearly all cells fall in
the range 0.25 to 4.0.